Impact of Benzo[a]pyrene-2‘-deoxyguanosine Lesions On Methylation Of DNA by SssI and HhaI DNA Methyltransferases †

ARTICLE *in* BIOCHEMISTRY · JUNE 2006

Impact Factor: 3.02 · DOI: 10.1021/bi0511639 · Source: PubMed

12 AUTHORS, INCLUDING:

Oksana M Subach
Albert Einstein College of Medicine
24 PUBLICATIONS **620** CITATIONS
SEE PROFILE

Maria V Darii
Lomonosov Moscow State University
9 PUBLICATIONS **55** CITATIONS
SEE PROFILE

Diana V Maltseva
Bioclinicum Research Centre
16 PUBLICATIONS **147** CITATIONS
SEE PROFILE

Francis Johnson
Stony Brook University
252 PUBLICATIONS **6,955** CITATIONS
SEE PROFILE

Impact of Benzo[*a*]pyrene-2′-deoxyguanosine Lesions On Methylation Of DNA by SssI and HhaI DNA Methyltransferases†

Oksana M. Subach,‡ Vladimir B. Baskunov,‡ Maria V. Darii,‡ Diana V. Maltseva,‡ Dmitrii A. Alexandrov,‡ Olga V. Kirsanova,‡,⊥ Alexander Kolbanovskiy,§ Marina Kolbanovskiy,§ Francis Johnson,|| Radha Bonala,|| Nicholas E. Geacintov,§ and Elizaveta S. Gromova*,‡

Chemistry Department, Moscow State University, Moscow, 119992, Russia, Department of Chemistry, New York University, 31 Washington Place, New York, New York 10003-5180, and Department of Pharmacological Sciences, State University of New York at Stony Brook, Stony Brook, New York 11794-3400

Received June 16, 2005; Revised Manuscript Received January 31, 2006

ABSTRACT: DNA damage caused by the binding of the tumorigen 7*R*,8*S*-diol 9*S*,10*R*-epoxide (B[*a*]PDE), a metabolite of bezo[*a*]pyrene, to guanine in CpG dinucleotide sequences could affect DNA methylation and, thus, represent a potential epigenetic mechanism of chemical carcinogenesis. In this work, we investigated the impact of stereoisomeric (+)- and (−)-*trans*-*anti*-B[*a*]P-N^2-dG adducts (B^+ and B^-) on DNA methylation by prokaryotic DNA methyltransferases M.SssI and M.HhaI. These two methyltransferases recognize CpG and GCGC sequences, respectively, and transfer a methyl group to the C5 atom of cytosine (C). A series of 18-mer unmethylated or hemimethylated oligodeoxynucleotide duplexes containing *trans*-*anti*-B[*a*]P-N^2-dG adducts was generated. The B^+ or B^- residues were introduced either 5′ or 3′ adjacent or opposite to the target 2′-deoxycytidines. The B[*a*]PDE lesions practically produced no effect on M.SssI binding to DNA but reduced M.HhaI binding by 1−2 orders of magnitude. In most cases, the benzo[*a*]pyrenyl residues decreased the methylation efficiency of hemimethylated and unmethylated DNA by M.SssI and M.HhaI. An absence of the methylation of hemimethylated duplexes was observed when either the (+)- or the (−)-*trans*-*anti*-B[*a*]P-N^2-dG adduct was positioned 5′ to the target dC. The effects observed may be related to the minor groove conformation of the bulky benzo[*a*]-pyrenyl residue and to a perturbation of the normal contacts of the methyltransferase catalytic loop with the B[*a*]PDE-modified DNA. Our results indicate that a *trans*-*anti*-B[*a*]P-N^2-dG lesion flanking a target dC in the CpG dinucleotide sequence on its 5′-side has a greater adverse impact on methylation than the same lesion when it is 3′ adjacent or opposite to the target dC.

DNA methylation is an epigenetic modification in the cellular genome. It is involved in various biological processes such as transcriptional silencing, genomic imprinting, regulation of development, chromatin structure, and DNA mismatch repair (*1*−*5*). In eukaryotes, methylation occurs at the 5-position of cytosine, predominantly when this nucleobase is part of CpG dinucleotide steps. The conversion of cytosine to 5-methylcytosine is catalyzed by DNA methyltransferases (MTases[1]) using *S*-adenosyl-L-methionine (AdoMet) as the methyl donor (AdoMet turns to *S*-adenosyl-L-homocysteine, AdoHcy) (*6*). In eukaryotes, the DNA methylation machinery involves several C5-cytosine MTases (C5 MTases) that act either on the unmethylated (de novo MTases) or hemimethylated (maintenance MTases) CpG sequences (*5*−*7*). The methylation patterns (the distribution of m^5dCpG within the genome) are stable in the adult genome for many cell generations (*5*−*7*). Aberrations in methylation patterns are observed in most if not all cancers, and tumor promotion is commonly associated with reduced levels of 5-methylcytosine (hypomethylation) relative to that of normal cells (*1, 8*). However, the higher levels of specific methylation of promoter regions in tumor suppressor genes (hypermethylation) silence the genes affected and, thus, may also lead to cancer (*1, 9*).

Chemical reactions of diol epoxides derived from the metabolic activation of polycyclic aromatic hydrocarbons (PAH) with DNA (*10, 11*) are known to cause mutations

† This research was supported by U. S. Public Health Service Grant No. TW05689 from the Fogarty International Center (New York University and Moscow State University), NIH Grant CA 099194 (New York University), NIEHS Grant ES-04068 (State University of New York at Stony Brook), and RFBR Grants 04-04-49488, 05-04-49690, and 04−04−49110 (Moscow State University).

* To whom correspondence should be addressed. Tel: +7 095 939 31 44. Fax: +7 095 939 31 81. E-mail: gromova@genebee.msu.ru.

‡ Moscow State University.

§ New York University.

|| State University of New York at Stony Brook.

⊥ Present Address: Engelhardt Institute of Molecular Biology, Russian Academy of Sciences, Moscow 117984, Russia.

[1] Abbreviations: AdoHcy, *S*-adenosyl-L-homocysteine; AdoMet, *S*-adenosyl-L-methionine; B[*a*]PDE, *r*7,*t*8-dihydroxy-*t*9,10-epoxy-7,8,9,-10-tetrahydrobenzo[*a*]pyrene; DTT, dithiothreitol; EMSA, electrophoretic mobility shift assay; FAM, 6(5)-carboxyfluorescein; M.SssI, SssI DNA methyltransferase; M.HhaI, HhaI DNA methyltransferase; MTase, DNA methyltransferase; PAGE, polyacrylamide gel electrophoresis; HPLC, high-performance liquid chromatography; T_m, melting temperature; K_d, dissociation constant; K_d^{app}, apparent dissociation constant; V_0, initial rate of methylation; V_{max}, maximal rate of methylation; k_{cat}, multiple turnover rate constant; k_{chem}, single turnover rate constant; TRD, target recognition domain.

10.1021/bi0511639 CCC: $33.50
Published on Web 04/18/2006

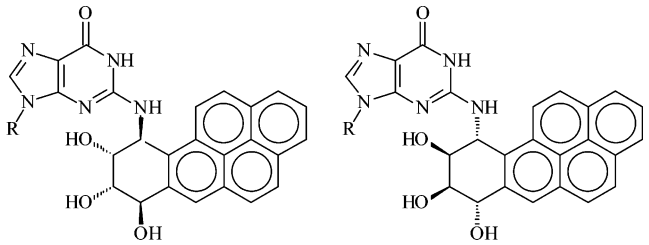

FIGURE 1: Chemical structures of the (+)- and (−)-*trans-anti*-B[*a*]P-N^2-dG adducts.

that can lead to the initiation of tumorigenesis. Benzo[*a*]pyrene (*12*), one of the most widely studied environmental PAH compounds, is metabolized in vivo to genotoxic 7,8-diol 9,10-epoxides (B[*a*]PDE) with an anti-orientation of the 7-hydroxyl and 9,10 epoxide groups. The (+)-7*R*,8*S*,9*S*,10*R* enantiomer [(+)-*anti*-B[*a*]PDE] is highly tumorigenic in animal models (*13*), whereas the (−)-7*S*,8*R*,9*R*,10*S* enantiomer [(−)-*anti*-B[*a*]PDE] is not. Both forms of B[*a*]PDE bind covalently to DNA by the nucleophilic attack of the N^2- or N^6-exocyclic amino groups of guanine or adenine, respectively, at the C10 position of the B[*a*]PDE molecule. Guanine is the major target of reaction, occurring mainly by the trans opening of the epoxide ring, thus producing the (+)- and (−)-*trans-anti*-B[*a*]P-N^2-dG adducts (*14*) (Figure 1). In cellular environments, the B[*a*]P-DNA adducts are removed by nucleotide excision repair, the only efficient system for the removal of such bulky lesions (reviewed in ref *15*). The repair of *trans-anti*-B[*a*]P-N^2-dG adducts by cell free extracts from human cells is relatively slow (*16*). Lesions that escape repair may block DNA replication and transcription or may be misread in an error-prone manner. The impact of B[*a*]PDE-damaged DNA on the function of topoisomerases (*17*), T7 RNA polymerase (*18*), human DNA polymerases (*19*, *20*), and transcription factor binding (*21*−*24*) have been studied.

The B[*a*]P-N^2-dG lesions are formed efficiently at the guanine residue in CpG sequence contexts (*25*) that are recognition sites of mammalian MTases. The efficiency of such damage is enhanced in the presence of m^5dC instead of dC in 5′-CpG targets (*25*−*27*). Such damage in the promoter region of a gene may disturb the normal functioning of MTases and change the genomic methylation pattern. In earlier publications, the methylation catalyzed by mammalian MTases and by M.HpaII of DNA randomly modified by reaction with B[*a*]PDE was reported (*28*−*31*). The B[*a*]P-DNA adducts were found to inhibit methylation in a manner that depended on the levels of modification. Recently, we reported that the prokaryotic MTase EcoRII is able to bind to DNA sequences with (+)- and (−)-*trans-anti*-B[*a*]P-N^2-dG adducts positioned within the EcoRII recognition sequence (CC(A/T)GG), but its catalytic activity is either significantly diminished or entirely blocked (*32*). The CC(A/T)GG sequence, in addition to the CpG sequences, was found to be a target of mammalian MTases (*33*, *34*).

The objective of this work was to examine how the C5-cytosine methylation in CpG and GCGC sequences is impacted by (+)- and (−)-*trans-anti*-B[*a*]P-N^2-dG adducts (Figure 1). We used site-specifically modified oligonucleotide duplexes with single (+)- and (−)-*trans-anti*-B[*a*]P-N^2-dG adducts to study the effects of stereochemistry and adduct position within the DNA substrate on methylation catalyzed by prokaryotic C5 MTases SssI and HhaI. We chose M.SssI for these studies because it is a unique prokaryotic MTase that shares specificity with mammalian MTases and the biochemically and crystallographically characterized M.HhaI. In fact, prokaryotic C5 MTases and the catalytic domains of mammalian MTases exhibit high sequence homologies and structural similarities (*6*), and the mechanisms of methyl transfer appear to be similar in all C5 MTases, including mammalian MTases (*35*, *36*).

The characteristics of M.SssI and M.HhaI have been studied previously. The prokaryotic MTase SssI from the bacterium *Spiroplasma* recognizes CpG sequences in DNA and methylates the C5 position of the cytosine residue within this sequence (*37*). A biologically active hybrid MTase containing the *N*-terminal regulatory domain of the mammalian Dnmt1 and most of the coding sequence of the M.SssI replacing the *C*-terminal catalytic domain of Dnmt1 has been constructed (*38*). Recently, a computer model of the ternary M.SssI·DNA·AdoHcy complex was generated (*39*). On the basis of this model, it was suggested that the part of the target recognition domain of M.SssI that is responsible for its direct interactions with the DNA recognition sequence, resembled the corresponding part of the target recognition domain of the CpG-specific mammalian MTase Dnmt2 (*39*). Taken together, these findings suggest that M.SssI is a good model for studying the mechanism of interaction of CpG-specific mammalian MTases with DNA. M.HhaI is a DNA C5-cytosine MTase, a component of a type II restriction-modification system from *Haemophilus haemolyticus*, which modifies the inner cytosine in the double-stranded sequence 5′-GCGC-3′. M.HhaI is one of the most extensively studied MTases. Various crystal structures of this enzyme in binary complexes with AdoMet or in ternary complexes with AdoMet (or AdoHcy) and with different DNA substrates have been solved (*40*−*42*). The kinetic and catalytic mechanisms of M.HhaI have been thoroughly characterized (*40*, *43*−*45*), and molecular dynamics simulations were also performed (*42*, *46*). Biochemical and structural studies of M.HhaI have significantly contributed to an understanding of the mechanism of C5-cytosine methylation (*40*).

It is shown here that the MTases SssI and HhaI are capable of binding to recognition sequences with B[*a*]P-N^2-dG adducts. Both M.SssI and M.HhaI methylate such modified sequences less efficiently than their unmodified counterparts. When the *trans-anti*-B[*a*]P-N^2-dG lesions are positioned at the 5′-side of the target cytosine in the hemimethylated duplex, they have a much more profound impact on DNA methylation than when the same lesions are present at other positions. The results obtained indicate that B[*a*]P-DNA damage is more critical to the methylation of hemimethylated DNA rather than unmethylated DNA sequences.

EXPERIMENTAL PROCEDURES

Chemicals and Enzymes. AdoMet and AdoHcy were purchased from Sigma (St. Louis, MO). [CH_3-^{3}H]−AdoMet (77 Ci/mmole, 13 μM) was from Amersham Biosciences (Little Chalfont, U.K.). [γ-^{32}P]-ATP (1000 Ci/mmole) was purchased from Izotop (Obninsk, Russia). DNA methyltransferase SssI (4000 U/mL) was purchased from New England BioLabs (Beverly, MA). Also, we used His_6-tagged

Table 1: Oligodeoxynucleotide Sequences Synthesized[a]

GCG	5′-GAGCCAAGCGCACTCTGA
CGC	5′-TCAGAGTGCGCTTGGCTC
GMG	5′-GAGCCAAGMGCACTCTGA
CGM	5′-TCAGAGTGMGCTTGGCTC
FAM-CGC	5′-FAM-TCAGAGTGCGCTTGGCTC
FAM-CGM	5′-FAM-TCAGAGTGMGCTTGGCTC
B^-CG	5′-GAGCCAAB^-CGCACTCTGA
B^+CG	5′-GAGCCAAB^+CGCACTCTGA
GCB^-	5′-GAGCCAAGCB^-CACTCTGA
GCB^+	5′-GAGCCAAGCB^+CACTCTGA
GMB^-	5′-GAGCCAAGMB^-CACTCTGA
GMB^+	5′-GAGCCAAGMB^+CACTCTGA

[a] M represents m^5dC; $B^{+/-}$: (+/−)-trans-*anti*-B[*a*]P-N^2-dG; and FAM: 5(6)-carboxyfluorescein.

M.SssI (6.7 μM). To obtain His_6-tagged M.SssI, an appropriate hybrid plasmid was produced (Darii, M. V., Drutsa, V. L., Kirsanova O. V., Kochetkov, S. N., Gromova E. S., unpublished results) using the vector pCAL7 provided by New England BioLabs (Beverly, MA). The kinetic parameters determined with wild type or His_6-tagged M.SssI were practically identical in value. DNA methyltransferase HhaI (4.4 mg/mL) was kindly provided by S. Klimasauskas (Vilnius, Lithuania). The MTases were found to be homogeneous on 12% polyacrylamide gels in the presence of 0.1% SDS. T4 polynucleotide kinase was obtained from MBI Fermentas (Vilnius, Lithuania). Buffers A−F were prepared using Milli-Q water. A: 10 mM Tris-HCl (pH 7.9), 50 mM NaCl; B: buffer A containing 1 mM DTT; C: buffer B containing 0.1 mg/mL acetylated bovine serum albumin; D: 50 mM Tris-HCl (pH 7.5), 50 mM NaCl, 10 mM EDTA, and 5 mM 2-mercaptoethanol; E: 50 mM Tris-HCl (pH 7.5), 50 mM NaCl, 10 mM EDTA, 5 mM 2-mercaptoethanol, and 0.2 mg/mL acetylated bovine serum albumin; F: 50 mM Tris-H_3BO_3 (pH 8.3) and 2 mM EDTA.

Oligodeoxynucleotides. The sequences of the oligodeoxynucleotides employed are summarized in Table 1. The complementary oligodeoxynucleotide strands GCG and CGC were purchased from IDT (Coralville, IA). The 5-methylcytosine containing oligodeoxynucleotides GMG and CGM and the fluorescein-labeled oligodeoxynucleotide FAM-CGC were synthesized by standard automated synthesis methods. The fluorescein label was introduced at the 5′-end of the oligodeoxynucleotide by means of an aminoalkyl linker containing six methylene groups.

The site-specifically modified oligodeoxynucleotides B^-CG, B^+CG, GCB^-, and GCB^+ contained single (+)- and (−)-*trans*-*anti*-B[*a*]P-N^2-dG lesions (B^+ and B^-, Figure 1 and Table 1) at either the 5′-side or the 3′-side 2′-deoxyguanosine within the GCGC nucleotide sequence in the 5′-GAGCCAAGCGCACTCTGA oligodeoxynucleotide. They were synthesized by automated DNA synthesis methods utilizing the appropriate 5′-*O*-DMTr-3′-*O*-phosphoroamidites derived from racemic mixtures of the 7*R*,8*S*,9*S*,10*R* and 7*S*,8*R*,9*R*,-10*S* enantiomers of B[*a*]PDE (*47*). The pairs of diastereomeric oligodeoxynucleotides were separated by reversed-phase HPLC utilizing an X Terra C18 column (Waters, Milford, MA).

Oligodeoxynucleotides GMB^- and GMB^+ were obtained by methylation of the hemimethylated oligodeoxynucleotide duplexes GCB^-/CGM and GCB^+/CGM (Table 2) by M.SssI, followed by the separation of the strands in denaturing polyacrylamide gel. To obtain duplexes GCB^-/CGM and GCB^+/CGM, either oligodeoxynucleotide GCB^- (2.5 nmol) or oligodeoxynucleotide GCB^+ (2.5 nmol) were annealed with the complementary strand CGM (2.6 nmol) in 440 μL of buffer A by heating the sample to 80 °C, followed by slow cooling to 20 °C. The duplexes obtained (3.1 μM) were methylated by M.SssI (17 nM) in buffer B containing AdoMet (160 μM). After 1 h of incubation at 37 °C, additional aliquots of M.SssI (17 nM) were added, and the reaction mixtures were incubated for 2 h. AcONa (0.3 M), EDTA (1 mM), and phenol/chloroform/isoamyl alcohol mixture (300 μL) were added to the reaction mixtures, and after extraction, the aqueous fractions were separated. DNA duplexes were precipitated from solution by ethanol and loaded onto denaturing 20% polyacrylamide gels with 7 M urea to separate the oligodeoxynucleotides, GMB^- or GMB^+, from the complementary strand, CGM. The compositions of the modified sequences were verified by mass spectrometry using a Bruker Daltonics OmniFlex or Reflex IV MALDI-TOF MS instruments (Bruker, Billerica, MA). A MALDI-TOF mass spectrometry analysis of GMB^- and GMB^+ revealed masses that are 14 Da higher than those of the unmethylated B[*a*]PDE-modified strands. MALDI-TOF mass spectra signals corresponding to the starting GCB^- or GCB^+ oligodeoxynucleotide were not observed. To ensure that all target cytosines were converted to the 5-methylcytosines, the purified oligodeoxynucleotides GMB^- or GMB^+ were annealed with the complementary strand CGM. There was no [CH_3-^{3}H] incorporation into these duplexes when tested for methylation by M.SssI in the presence of [CH_3-^{3}H]−AdoMet, and thus, the B[*a*]PDE-modified strands did not contain any unmethylated target cytosine residues.

All oligodeoxynucleotides were further purified by electrophoresis on denaturing 20% polyacrylamide gels and desalted by passing the solutions through C18 Sep-Pack cartridges (Waters, Milford, MA). The sequences were labeled via the standard ^{32}P-5′-phosphorylation of oligodeoxynucleotides using T4 polynucleotide kinase and [γ-^{32}P]-ATP.

Oligodeoxynucleotide concentrations were estimated spectrophotometrically. The extinction coefficients (ϵ_{260}) of unmodified and B[*a*]PDE-modified oligonucleotides were calculated as described (*32*, *48*).

Fluorescence Polarization Measurements. Fluorescence polarization measurements involving the labeled oligodeoxynucleotide duplex GCG/FAM−CGC were performed at 25 °C by means of a Beacon 2000 Fluorescence Polarization System (PanVera) with excitation at 488 nm and emission at 535 nm using 10 × 75 mm borosilicate sample glass test tubes. The polarization (*P*) was defined in terms of the vertical (I_v) and horizontal (I_h) emission components and the expression

$$P = \frac{(I_v - GI_h)}{(I_v + GI_h)}$$

where *G* is an instrumental correction factor. The reaction mixtures were allowed to equilibrate, and the polarization values were determined from at least three independent measurements.

Determination of the Amount of the Active Form of M.SssI and M.HhaI. M.SssI (commercial preparation, 0.234 U/μL

Table 2: Properties of the B[*a*]PDE-Modified Oligodeoxynucleotide Duplexes as Substrates of M.SssI

Designation	DNA duplex [a]	K_d, nM	k_{cat}, min^{-1}	k_{chem}, min^{-1}
GCG/CGC	5′GAGCCAAG**C**G**C**ACTCTGA 3′CTCGGTTC**G**C**G**TGAGACT	5.6 ± 0.2 [b]	4.3 ± 0.5	-
B⁻CG/CGC	5′GAGCCAAB⁻**C**G**C**ACTCTGA 3′CTCGGTTC **G**C**G**TGAGACT	6.7 ± 1.3	0.2 ± 0.1	-
B⁺CG/CGC	5′GAGCCAAB⁺**C**G**C**ACTCTGA 3′CTCGGTTC **G**C**G**TGAGACT	8.2 ± 1.7	0.5 ± 0.1	-
GCB⁻/CGC	5′GAGCCAAG**C**B⁻CACTCTGA 3′CTCGGTTC**G**C **G**TGAGACT	9.9 ± 2.0	0.9 ± 0.1	-
GCB⁺/CGC	5′GAGCCAAG**C**B⁺CACTCTGA 3′CTCGGTTC**G**C **G**TGAGACT	7.5 ± 1.4	2.4 ± 0.4	-
GCG/CGM	5′GAGCCAAG**C**G**C**ACTCTGA 3′CTCGGTTC**GM**GTGAGACT	5.3 ± 0.3	2.3 ± 0.2	4.4 ± 1.0
B⁻CG/CGM	5′GAGCCAAB⁻**C**G**C**ACTCTGA 3′CTCGGTTC **GM**GTGAGACT	9.8 ± 1.9	< 0.0005	< 0.002
B⁺CG/CGM	5′GAGCCAAB⁺**C**G**C**ACTCTGA 3′CTCGGTTC **GM**GTGAGACT	24.4 ± 4.9	< 0.0005	< 0.002
GCB⁻/CGM	5′GAGCCAAG**C**B⁻CACTCTGA 3′CTCGGTTC**GM** GTGAGACT	5.3 ± 1.0	1.9 ± 0.1	2.5 ± 0.2
GCB⁺/CGM	5′GAGCCAAG**C**B⁺CACTCTGA 3′CTCGGTTC**GM** GTGAGACT	7.5 ± 1.5	3.6 ± 0.2	3.5± 0.2
GMG /CGC	5′GAGCCAAG**MG**CACTCTGA 3′CTCGGTTC**G**C**G**TGAGACT	5.0 ± 1.0	1.9 ± 0.2	-
GMB⁻/CGC	5′GAGCCAAG**MB**⁻CACTCTGA 3′CTCGGTTC**G**C **G**TGAGACT	8.9 ± 1.7	0.32 ± 0.02	0.3 ± 0.1
GMB⁺/CGC	5′GAGCCAAG**MB**⁺CACTCTGA 3′CTCGGTTC**G**C **G**TGAGACT	5.9 ± 1.2	1.5 ± 0.1	1.7 ± 0.2

[a] The M.SssI recognition sequence is shown in bold. The target cytosines are underlined. Both target cytosines in duplexes GCG/CGC, B⁻CG/CGC, B⁺CG/CGC, GCB⁻/CGC, and B⁺CG/CGC can be methylated. [b] The K_d value determined for the M.SssI·GCG/FAM−CGC·AdoHcy complex was taken to be equal to the K_d value of the M.SssI·GCG/CGC·AdoHcy complex.

or His_6-tagged protein, 6.7 μM as determined by a Bradford assay) was incubated with ^{32}P-labeled oligodeoxynucleotide duplex GCG/CGC (60 nM) and varying amounts of the unlabeled oligodeoxynucleotide duplex GCG/CGC (0−400 nM) in buffer C containing AdoHcy (1 mM) and 8% glycerol at room temperature for 5 min and at 0 °C for 5 min. The reaction mixtures were analyzed by nondenaturing 8% PAGE in 0.5× buffer F. Here, and in all other gel electrophoresis experiments, the gels were analyzed by autoradiography utilizing a Molecular Dynamics Phosphorimager (Amersham Biosciences, Little Chalfont, U.K.) with ImageQuant 5.0 software. Here, and elsewhere, when radioactivity gels were processed, the radioactivity of free (cpm_{free}), total (cpm_{total}) and bound ($cpm_{bound} = cpm_{total} - cpm_{free}$) DNA were determined. The total oligodeoxynucleotide duplex concentration (^{32}P-labeled and unlabeled) was plotted versus the ratio (cpm_{total})/(cpm_{bound}) (Supporting Information, Figure 1S) as described in ref *49*. The concentration of active protein was determined from the tangent of the angle between the straight line representing the dependence of the total DNA concentration versus cpm_{total}/cpm_{bound} and the abscissa axis. The concentration of the active form of M.SssI was 332 ± 5 nM (commercial preparation) or 338 ± 22 nM (His_6-tagged protein).

The amount of the active form of M.HhaI was calculated using binding-site titration. The GCG/FAM−CGC duplex (3 nM) and AdoHcy (0.1 mM) were preincubated in 0.5 mL of buffer E. M.HhaI (120 μM according to personal communication from S. Klimasauskas) was added in 0.1−0.3 nM aliquots to a final concentration of 5 nM, and the fluorescence polarization was measured. The fluorescence polarization was plotted versus the total M.HhaI concentration (data not shown), and the plot was processed as described in ref *32*. The concentration of the active form of M.HhaI was found to be 120 ± 10 μM.

Direct Titrations. (a) Determination of the K_d value for the M.SssI·GCG/FAM−CGC·AdoHcy Complex by Fluorescence Polarization Measurements. Duplex GCG/FAM−CGC (1 nM) and AdoHcy (1 mM) were preincubated in 0.5 mL of buffer C, and the fluorescence polarization value of the oligodeoxynucleotide duplex prior to the addition of M.SssI (P_0) was measured. M.SssI was added in 2.5 nM aliquots to a final concentration of 29.6 nM, and the fluorescence polarization was measured. The K_d value was calculated by fitting the data to the following equation, which is based on a standard bimolecular binding equilibrium (*50*)

$$P = P_0 + \frac{P_{max} - P_0}{2[S]_0}([S]_0 + [E]_0 + K_d - \sqrt{([S]_0 + [E]_0 + K_d)^2 - 4\cdot[E]_0\cdot[S]_0}) \quad (1)$$

where P is the measured polarization value at any particular point in the titration curve, P_0 and P_{max} are polarization values of the free and fully bound GCG/FAM−CGC oligodeoxynucleotide duplexes, $[E]_0$ and $[S]_0$ are total concentrations

of the enzyme and the fluorescence-emitting duplex GCG/FAM−CGC, respectively.

(b) Determination of the K_d Value for the M.SssI·GCG/CGC·AdoHcy Complex by EMSA. ^{32}P-labeled duplex GCG/CGC (1 nM) was incubated in the presence of 1 mM AdoHcy with varying M.SssI concentrations (0−53 nM) in buffer C containing 8% glycerol at room temperature for 5 min and at 0 °C for 5 min. The reaction mixtures were analyzed by nondenaturing 8% PAGE in 0.5× buffer F. The ratio $(cpm_{bound})/(cpm_{total})$ was calculated and plotted versus the total protein concentration. The K_d value was calculated by fitting the data to the following equation, which is based on a standard bimolecular binding equilibrium (51)

$$\frac{cpm_{bound}}{cpm_{total}} = \frac{[ES]}{[S]_0} = \frac{1}{2[S]_0}([S]_0 + [E]_0 + K_d - \sqrt{([S]_0 + [E]_0 + K_d)^2 - 4\cdot[E]_0\cdot[S]_0}) \quad (2)$$

where $[S]_0$ and $[E]_0$ are the total DNA and M.SssI concentrations, respectively.

Equilibrium Competition Experiments. K_d determination by EMSA. In the case of the M.SssI·B[*a*]P-DNA·AdoHcy complexes, one of the reference ^{32}P-labeled oligodeoxynucleotide duplexes GCG/CGC, GCG/CGM, or GMG/CGC (100 nM) was mixed with increasing concentrations of B[*a*]-PDE-modified competitor oligodeoxynucleotide duplex (0−650 nM) in buffer C containing 8% glycerol and AdoHcy (1mM). M.SssI was added to a final concentration of 50 nM, and the samples were incubated. The reference oligodeoxynucleotide duplex GCG/CGC was used in reactions with competitors B^-CG/CGC, B^+CG/CGC, GCB^-/CGC, and GCB^+/CGC; duplex GCG/CGM was used in equilibrium binding reactions with competitors B^-CG/CGM, B^+CG/CGM, GCB^-/CGM, and GCB^+/CGM, and duplex GMG/CGC was used in reactions with competitors GMB^-/CGC and GMB^+/CGC.

In the case of M.HhaI·B[*a*]P-DNA·AdoHcy complexes, the reference ^{32}P-labeled oligodeoxynucleotide duplex GCG/CGM (2 nM) was mixed with increasing concentrations of each B[*a*]PDE-modified competitor oligodeoxynucleotide duplex (0−12 μM) in buffer E containing 8% glycerol and AdoHcy (0.1 mM). M.HhaI was added to a final concentration of 1 nM, and the samples were equilibrated at 37 °C for 5 min and then at 0 °C for 5 min.

The samples containing a ^{32}P-labeled reference oligodeoxynucleotide duplex, an unlabeled B[*a*]PDE-modified competitor duplex, and SssI or HhaI MTase were analyzed by nondenaturing 8% PAGE in 0.5× buffer F. The ratio of DNA radioactivity cpm_{bound}/cpm_{total} was plotted versus the competitor DNA concentration.

Equation 3 was derived on the basis of the bimolecular binding equilibrium (the derivation is outlined in Supporting Information). The values of $k = K_d/K_d^r$ were determined from the best fits of eq 3 to the experimental data points.

$$\frac{cpm_{bound}}{cpm_{free}} = \frac{1}{2[S]_0(1-1/k)}\{[S]_0 + [E]_0 + ([C]_0 - [E]_0)/k - \sqrt{[([S]_0 + [E]_0 + (1/k)([C]_0 - [E]_0))^2 - 4[S]_0[E]_0(1-1/k)]}\} \quad (3)$$

where $[E]_0$, $[S]_0$, and $[C]_0$ are the total concentrations of the enzyme, the ^{32}P-labeled oligodeoxynucleotide duplex, and the unlabeled B[*a*]PDE-modified competitor oligodeoxynucleotide duplex; K_d^r and K_d are dissociation constants for MTase·reference DNA·AdoHcy and MTase·B[*a*]P-DNA·AdoHcy complexes.

The $k = K_d/K_d^r$ ratio specifies the relative binding affinity of the competitor damaged DNA, to the MTase as compared to that of the reference DNA.

In the case of M.HhaI, we used the ratio k to compare the relative binding affinity of B[*a*]PDE-modified and unmodified GCG/CGC DNA duplexes to M.HhaI.

For M.SssI, the values of K_d were calculated by dividing the values of K_d^r by the experimental values of k. The K_d^r for the M.SssI·GCG/CGC·AdoHcy complex was assumed (*50*) to be equal to the dissociation constant for the M.SssI·GCG/FAM−CGC·AdoHcy complex determined by direct titration (see above). The K_d^r value for the M.SssI·GCG/CGM·AdoHcy and M.SssI·GMG/CGC·AdoHcy complexes were obtained by the competitive binding of the unlabeled duplex GCG/CGM (or GMG/CGC) and the ^{32}P-labeled oligodeoxynucleotide duplex GCG/CGC with M.SssI. The experimental procedures were the same as those used in the determination of K_d for M.SssI·damaged DNA·AdoHcy complexes.

Equilibrium Competition Experiments. Kinetics of Complex Formation of M.SssI and M.HhaI with DNA. Fluorescein-labeled and otherwise unmodified GCG/FAM−CGC (100 nM in the case of M.SssI or 2 nM in the case of M.HhaI) and varying concentrations of B[*a*]PDE-modified oligodeoxynucleotide duplex (0−800 nM) were preincubated in buffer C containing 1 mM AdoHcy at 25 °C, and the fluorescence polarization of each sample (P_0) was measured. Subsequently, either M.SssI (20 nM) or M.HhaI (1 nM) was added, and each of these incubation mixtures was vortexed (∼10 s). The fluorescence polarization was then measured at 10 s intervals during 17 min.

Methylation Assay. The efficiency of methylation was monitored by the radioactivity of tritium (CH_3-^{3}H) incorporated into the oligodeoxynucleotide duplexes (*52*). The reactions were carried out in buffer B for M.SssI or D for M.HhaI, containing one of the oligodeoxynucleotide duplexes listed in Tables 2 and 3, M.SssI (18 nM) or M.HhaI (5 nM) and [CH_3-^{3}H]−AdoMet (1.3 μM). Oligodeoxynucleotide duplex concentrations were 1−2 μM in the M.SssI reactions and 100−500 nM in the M.HhaI reactions. These reactions were started either by adding [CH_3-^{3}H]−AdoMet (in the case of M.SssI) or the enzyme (in the case of M.HhaI). After a 0.5−15 min incubation time at 37 °C, aliquots of the reaction mixtures were pipetted onto DE-81 paper disks (Whatman, Brentford, U.K.) and treated as described (*53*). The amounts of methylated DNA were computed as described (*52*).

Single-Turnover Assays. Reactions of 1.3 μM M.SssI (or 1 μM M.HhaI), 100 nM DNA, and 1.3 μM [CH_3-^{3}H]−AdoMet were performed in buffer B (or D) at 37 °C. The reactions were started by the addition of AdoMet or MTase in the case of M.SssI or M.HhaI, respectively. The aliquots (4.5 μL) were quenched manually into 4μL of a 2 M HCl solution with 6−8 s time intervals. In the case of oligodeoxynucleotide duplexes BCG/CGM, the reactions were quenched after incubation for 0.5, 3, 5, 10, 15, and 120 min (for M.SssI) or for 0.5, 1, 2, 3, 5, 20, 30, 40, and 60 min (for M.HhaI). The aliquots were neutralized by 4 μL of 2 M

Table 3: Properties of the B[*a*]PDE-Modified Oligodeoxynucleotide Duplexes as Substrates of M.HhaI

Designation	DNA duplex [a]	k [b]	k_{cat}, min^{-1}	k_{chem}, min^{-1}
GCG/CGC	5′GAGCCAA**G**C**G**C**A**CTCTGA 3′CTCGGTT**C**G**C**G**T**GAGACT	1.2 ± 0.3	3.7 ± 0.3	-
B$^-$CG/CGC	5′GAGCCAA**B**$^-$C**G**C**A**CTCTGA 3′CTCGGTT**C** G**C**G**T**GAGACT	4.1 ± 1.2	2.3 ± 0.3	-
B$^+$CG/CGC	5′GAGCCAA**B**$^+$C**G**C**A**CTCTGA 3′CTCGGTT**C** G**C**G**T**GAGACT	17.4 ± 4.6	2.7 ± 0.1	-
GCB$^-$/CGC	5′GAGCCAA**G**C**B**$^-$**C**ACTCTGA 3′CTCGGTT**C**G**C** G**T**GAGACT	55.7 ± 15.5	0.9 ± 0.1	-
GCB$^+$/CGC	5′GAGCCAA**G**C**B**$^+$**C**ACTCTGA 3′CTCGGTT**C**G**C** G**T**GAGACT	39.3 ± 13.8	1.3 ± 0.4	-
GCG/CGM	5′GAGCCAA**G**C**G**C**A**CTCTGA 3′CTCGGTT**C**G**M**G**T**GAGACT	1.0 ± 0.4	3.7 ± 0.1	≥16 [c]
B$^-$CG/CGM	5′GAGCCAA**B**$^-$C**G**C**A**CTCTGA 3′CTCGGTT**C** G**M**G**T**GAGACT	17.2 ± 1.7	0.0045 ± 0.0005	0.008 ± 0.002
B$^+$CG/CGM	5′GAGCCAA**B**$^+$C**G**C**A**CTCTGA 3′CTCGGTT**C** G**M**G**T**GAGACT	103.0 ± 9.8	0.020 ± 0.002	0.040 ± 0.005
GCB$^-$/CGM	5′GAGCCAA**G**C**B**$^-$**C**ACTCTGA 3′CTCGGTT**C**G**M** G**T**GAGACT	80.9 ± 11.8	0.4 ± 0.1	0.83 ± 0.06
GCB$^+$/CGM	5′GAGCCAA**G**C**B**$^+$**C**ACTCTGA 3′CTCGGTT**C**G**M** G**T**GAGACT	44.9 ± 19.3	1.2 ± 0.1	4.5 ± 0.8
GMG /CGC	5′GAGCCAA**G**M**G**C**A**CTCTGA 3′CTCGGTT**C**G**C**G**T**GAGACT	-	3.6 ± 0.3	-
GMB$^-$/CGC	5′GAGCCAA**G**M**B**$^-$**C**ACTCTGA 3′CTCGGTT**C**G**C** G**T**GAGACT	43.4 ± 8.4	1.1 ± 0.1	1.4 ± 0.4
GMB$^+$/CGC	5′GAGCCAA**G**M**B**$^+$**C**ACTCTGA 3′CTCGGTT**C**G**C** G**T**GAGACT	33.9 ± 5.4	2.9 ± 0.1	5.1 ± 0.8

[a] The M.HhaI recognition sequence is shown in bold. The target cytosines are underlined. Both target cytosines in duplexes GCG/CGC, B$^-$CG/CGC, B$^+$CG/CGC, GCB$^-$/CGC, and B$^+$CG/CGC can be methylated. [b] The $k = K_d^{(app)}/K_d^{r(app)}$ value is the relative binding affinity of B[*a*]PDE-modified DNA (or unmodified GCG/CGC duplex) to M.HhaI as compared to that of the reference unmodified GCG/CGM (see Experimental Procedures). [c] Because, in the case of the unmodified substrate, the k_{chem} value was too fast to be measured, only the lower limit can be indicated.

NaOH, spotted onto DE-81 filters, and processed as described (*52*, *53*). The k_{chem} values were calculated from a nonlinear regression of the data according to the following equation

$$\frac{[MS]}{[S]_0} = 1 - \exp(-k_{chem}t) \quad (4)$$

where [MS] and $[S]_0$ are the concentrations of the methylated product and the total DNA, respectively. Equation 4 is based on the assumption of a pseudo-first-order methylation reaction rate ($[E]_0$, [AdoMet] $\gg$ $[S]_0$; $[E]_0$, $[S]_0 \gg K_d$).

RESULTS

Substrate Design. To determine the effects of the B[*a*]P-N^2-dG lesions on DNA methylation, we studied the sequence-specific recognition of the modified oligodeoxynucleotide duplexes by M.SssI and M.HhaI and the methylation reactions catalyzed by these enzymes. The length of the oligodeoxynucleotide duplexes was chosen to be 18 base pairs long, which is somewhat larger than the 16 bp DNA footprints of the HhaI and SssI MTases (*54*). Each oligodeoxynucleotide duplex contained overlapping recognition sites of M.HhaI (GCGC) and M.SssI (CpG) and, thus, was used as a substrate for both MTases (Tables 2 and 3). Stereoisomeric (+) or (−)-*trans*-*anti*-B[*a*]P-N^2-dG adducts (Figure 1) were substituted for one of the dG residues in the GCGC sequence either on the 5′-side of the methylation target dC (BCG/CGC and BCG/CGM, Tables 2 and 3) or on its 3′ side (GCB/CGC and GCB/CGM Tables 2 and 3), or opposite to it (GMB/CGC, Tables 2 and 3). Substituents were either within the SssI recognition sequence (GCB/CGC, GCB/CGM, and GMB/CGC), or adjacent to it on the 5′-side (BCG/CGC and BCG/CGM). Alternatively, the modified dG residues were located within the HhaI recognition sequence (BCG/CGC, BCG/CGM, GCB/CGC, GCB/CGM, and GMB/CGC). Both the unmethylated and hemimethylated oligodeoxynucleotide duplexes were studied. In unmethylated duplexes GCG/CGC, BCG/CGC, and GCB/CGC, both target cytosines in the SssI/HhaI recognition sequences can be methylated by MTases SssI or HhaI. The hemimethylated substrates contained m^5dC instead of the target dC in the neighborhood of B[*a*]P-N^2-dG (GMB/CGC) or in the complementary strand (BCG/CGM and GCB/CGM) (Tables 2 and 3). These sequences allowed us to evaluate the impact of the lesions B$^+$/B$^-$ positioned at different sites, either on the 5′- or 3′-sides of the target dC residues or in the complementary strand opposite to the individual target dC residues.

The oligodeoxynucleotides 5′-GAGCCAABCGCACTCTGA and 5′-GAGCCAAGCBCACTCTGA, representing the upper strand in oligodeoxynucleotide duplexes BCG/CGC,

GCB/CGC, BCG/CGM, and GCB/CGM (Tables 2 and 3), were synthesized by automated DNA synthesis methods. The two oligonucleotides containing either the (+)- or (−)-*trans-anti*-B[*a*]P-N^2-dG adducts were easily separated from one another and purified using reversed-phase HPLC (*47*). The oligodeoxynucleotides 5′-GAGCCAAGMB$^-$CACTCTGA and 5′-GAGCCAAGMB$^+$CACTCTGA, representing the upper strand in the oligodeoxynucleotide duplexes GMB/CGC (Tables 2 and 3), were obtained by methylation of oligonucleotides 5′-GAGCCAAGCB$^-$CACTCTGA and 5′-GAGCCAAGCB$^+$CACTCTGA within the oligodeoxynucleotide duplexes GCB$^-$/CGM and GCB$^+$/CGM by M.SssI, followed by the separation of the methylated strands using denaturing polyacrylamide gel electrophoresis (see Experimental Procedures). M.SssI is capable of efficiently transferring a methyl group to the B[*a*]PDE-modified strand of duplexes GCB$^-$/CGM and GCB$^+$/CGM (see below).

The melting curves of the B[*a*]PDE-modified oligodeoxynucleotide duplexes BCG/CGC and GCB/CGC were cooperative in all cases with the T_m values ranging from 61 to 63 °C, being only 3−5 °C lower than the T_m values of the unmodified duplex GCG/CGC. The T_m values of the hemimethylated B[*a*]PDE-modified oligodeoxynucleotide duplexes BCG/CGM, GCB/CGM, or GMB/CGC ranging from 61 to 65 °C, were 3−7 °C lower than that of duplex GCG/CGM. Further details are provided in Supporting Information, Table 1S.

Binding of M.SssI to Unmodified Oligodeoxynucleotide Duplexes GCG/FAM−CGC and GCG/CGC. The binding of M.SssI and M.HhaI to duplexes GCG/FAM−CGC and GCG/CGC as well as to the B[*a*]PDE-modified duplexes (see below) was performed in the presence of the cofactor analogue AdoHcy. In the case of C5 MTases, AdoHcy facilitates the formation of the specific complexes (55, 56).

First, the K_d value of the ternary M.SssI·unmodified DNA·AdoHcy complex was determined by the fluorescence polarization technique. This technique is a true equilibrium method because the attainment of equilibrium can be experimentally observed (Supporting Information), thus allowing for accurate determinations of K_d (50). Changes in the values of the fluorescence polarization, *P*, were easily detectable when aliquots of M.SssI were added to solutions of duplex GCG/FAM−CGC in the presence of AdoHcy (Figure 2). The K_d value of the M.SssI·GCG/FAM−CGC·AdoHcy complex was found to be 5.6 ± 0.2 nM. The FAM label does not interfere with the formation of the 18-mer DNA−protein complexes (32, 50). Therefore, it was assumed that the K_d value of the M.SssI·GCG/FAM−CGC·AdoHcy complex is equal to that of the M.SssI·GCG/CGC·AdoHcy complex. We also determined the K_d value of the ternary M.SssI·GCG/CGC·AdoHcy complex by direct titration of duplex GCG/CGC by M.SssI using EMSA (data not shown). The K_d value of the M.SssI·GCG/CGC·AdoHcy complex was found to be 7.4 ± 3.2 nM which correlates with the K_d value determined by the fluorescence polarization technique.

We were unable to obtain an accurate value of K_d for the M.HhaI·GCG/CGC·AdoHcy complex by a direct titration of duplex GCG/CGC with increasing enzyme concentrations. The experimental error associated with the dilution of the enzyme and the low radioactivity in the EMSA, or the low fluorescence signal in the fluorescence polarization experiments at low (picomolar) concentrations of DNA, prevented the accurate measurements of the small changes in these signals.

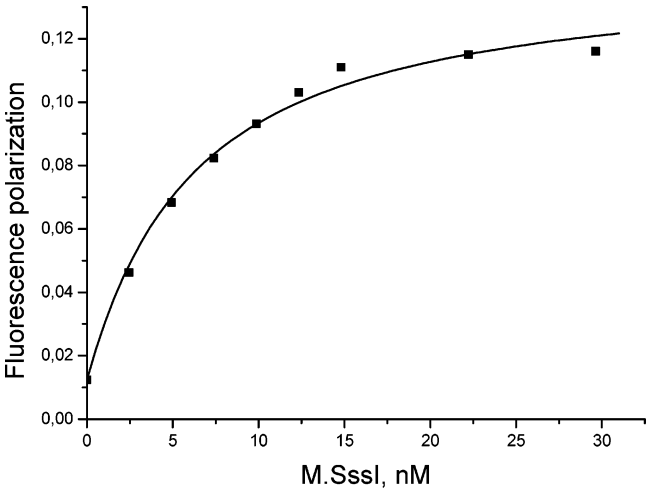

FIGURE 2: Direct titration of fluorescein-labeled oligodeoxynucleotide duplex GCG/FAM−CGC (1 nM) with M.SssI (0−30 nM) in the presence of AdoHcy (1 mM). The solid line represents a best fit to a simple binding isotherm and yields a K_d value of 5.6 ± 0.2 nM for the M.SssI·GCG/FAM−CGC·AdoHcy complex.

Binding of M.SssI and M.HhaI to B[a]PDE-modified Oligodeoxynucleotide Duplexes. To determine the binding affinities of M.SssI or M.HhaI to the B[*a*]PDE-modified oligodeoxynucleotide duplexes, we used an assay based on equilibrium competitive binding of the unlabeled B[*a*]PDE-modified and ^{32}P-labeled unmodified duplexes to MTase (57). The unlabeled B[*a*]PDE-modified DNA competed with the ^{32}P-labeled unmodified DNA for the DNA binding site in the MTase and reduced the amount of the MTase·^{32}P-labeled DNA·AdoHcy complex. The formation of the complexes was monitored by EMSA. Representative autoradiographs of such EMSA experiments for M.SssI and M.HhaI are depicted in Figures 3A and 4A, respectively. There is comparatively little material between the bands corresponding to the free DNA and protein-bound DNA, suggesting that there is no significant dissociation of the complexes during these EMSA experiments. The unlabeled duplex B$^+$CG/CGM competes with the ^{32}P-labeled duplex GCG/CGM for the DNA binding site in the MTase, and thus, the concentration of MTase·GCG/CGM·AdoHcy gradually diminishes as the concentration of the B$^+$CG/CGM is increased. The competition curves (Figures 3B−D and 4B−D) are characteristic of an equilibrium competition process (57).

The measurement of accurate K_d values by any method requires that equilibrium be attained when the fractions of free and protein-bound substrates are evaluated. We therefore monitored the kinetics of formation of the complexes of MTases with B[*a*]PDE-modified and unmodified duplexes by the fluorescence polarization method. Typical results are depicted in Supporting Information, Figure 2S. In all cases, the polarization value *P* increased with increasing time, and an apparent limiting value *P* was approached within ~10 min or less, suggesting that no further measurable changes in the concentrations of the complexes occurred. In the case of M.SssI, we were able to estimate the value of k_{-1} (5×10^{-3} s^{-1}) for the M.SssI·B[*a*]P-DNA·AdoHcy complexes by

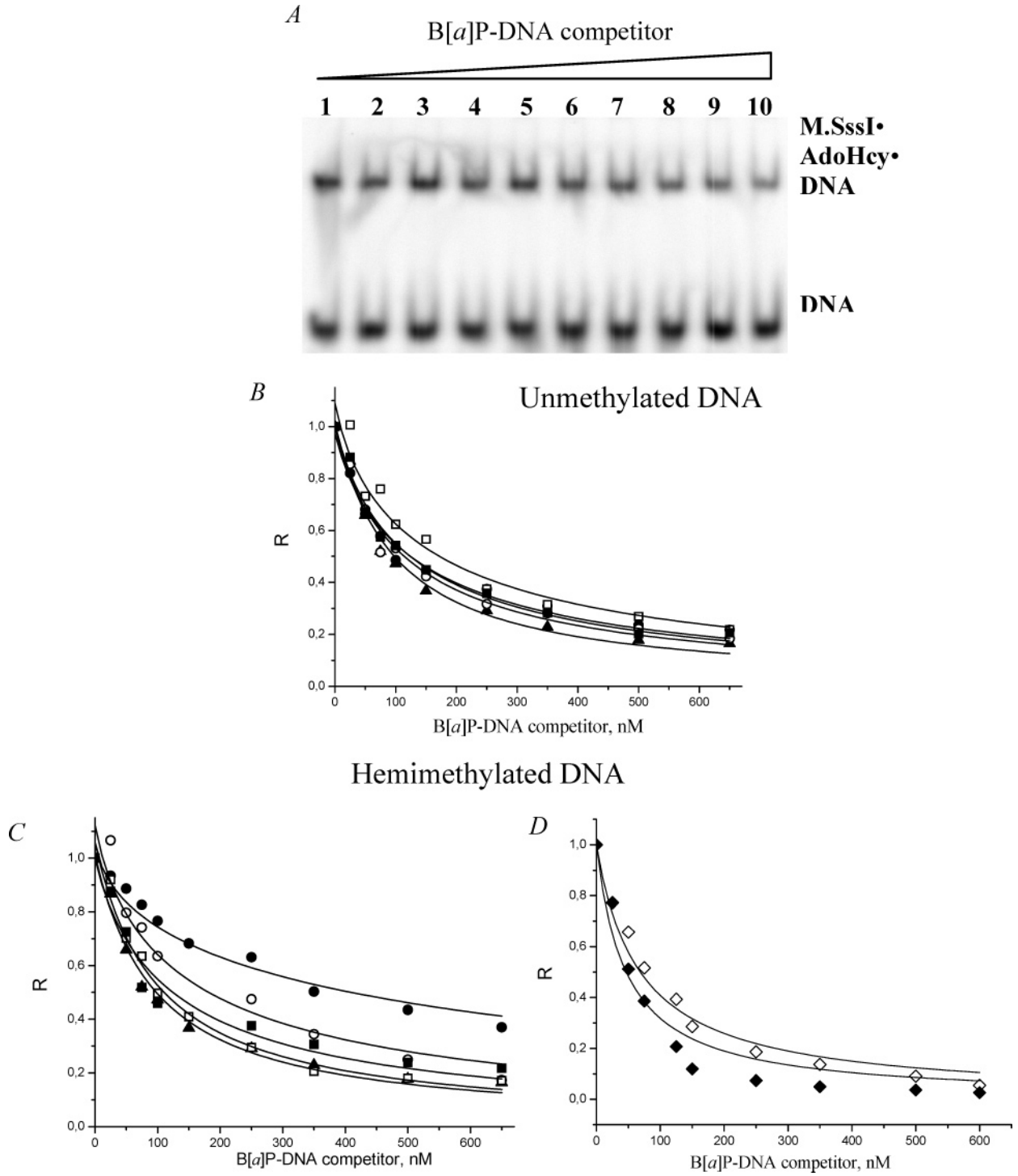

FIGURE 3: Competitive binding of B[*a*]PDE-modified oligodeoxynucleotide duplexes and unmodified oligodeoxynucleotide duplexes to M.SssI. (A) Autoradiograph of EMSA of binding of unlabeled B[*a*]PDE-modified duplex B^+CG/CGM and ^{32}P-labeled unmodified duplex GCG/CGM to M.SssI. GCG/CGM (100 nM) was mixed with increasing concentrations of competitor B^+CG/CGM (0, 25, 50, 75, 100, 150, 250, 350, 500, and 600 nM, numbered 1−10, respectively) and 50 nM M.SssI in buffer C containing 1 mM AdoHcy. *B*, *C*, and *D*. Equilibrium competition curves for M.SssI complexes with AdoHcy and ^{32}P-labeled duplexes GCG/CGC (B), GCG/CGM (C), or GMG/CGC (D) in the presence of increasing concentrations of the competitor B[*a*]PDE-modified duplexes. The relative fraction of bound ^{32}P-labeled DNA, *R*, is the ratio of the fraction of bound ^{32}P-labeled DNA in the presence of the competitor DNA (cpm_{bound}/cpm_{total}) to the fraction of bound ^{32}P-labeled DNA in the absence of the competitor DNA ($cpm_{bound}^0/cpm_{total}^0$). It was determined at different concentrations of the competitor DNA. B[*a*]PDE-modified duplexes: (B) GCG/CGC (▲), B^-CG/CGC (○), B^+CG/CGC (●), GCB$^-$/CGC (□), GCB$^+$/CGC (■); (C and D) GCG/CGM (▲), B^-CG/CGM (○), B^+CG/CGM (●), GCB$^-$/CGM (□), GCB$^+$/CGM (■), GMB$^-$/CGC (◊), and GMB$^+$/CGC (♦).

kinetic competition binding experiments (Figure 3S, Supporting Information), suggesting that true equilibrium was reached in the fluorescence polarization experiments on ~10 min time scales ($K_d = k_{-1}/k_1$, where k_1 and k_{-1} are association and dissociation rate constants of the binding of MTase with the DNA duplex). This allowed us to estimate the values of K_d for the M.SssI·B[*a*]P-DNA·AdoHcy complexes (Table 2). However, in the case of the analogous complexes with M.HhaI, the k_{-1} value of a 37-mer oligodeoxynucleotide duplex at 25 °C is known to be small (2.8×10^{-6} s^{-1}) (*44*),

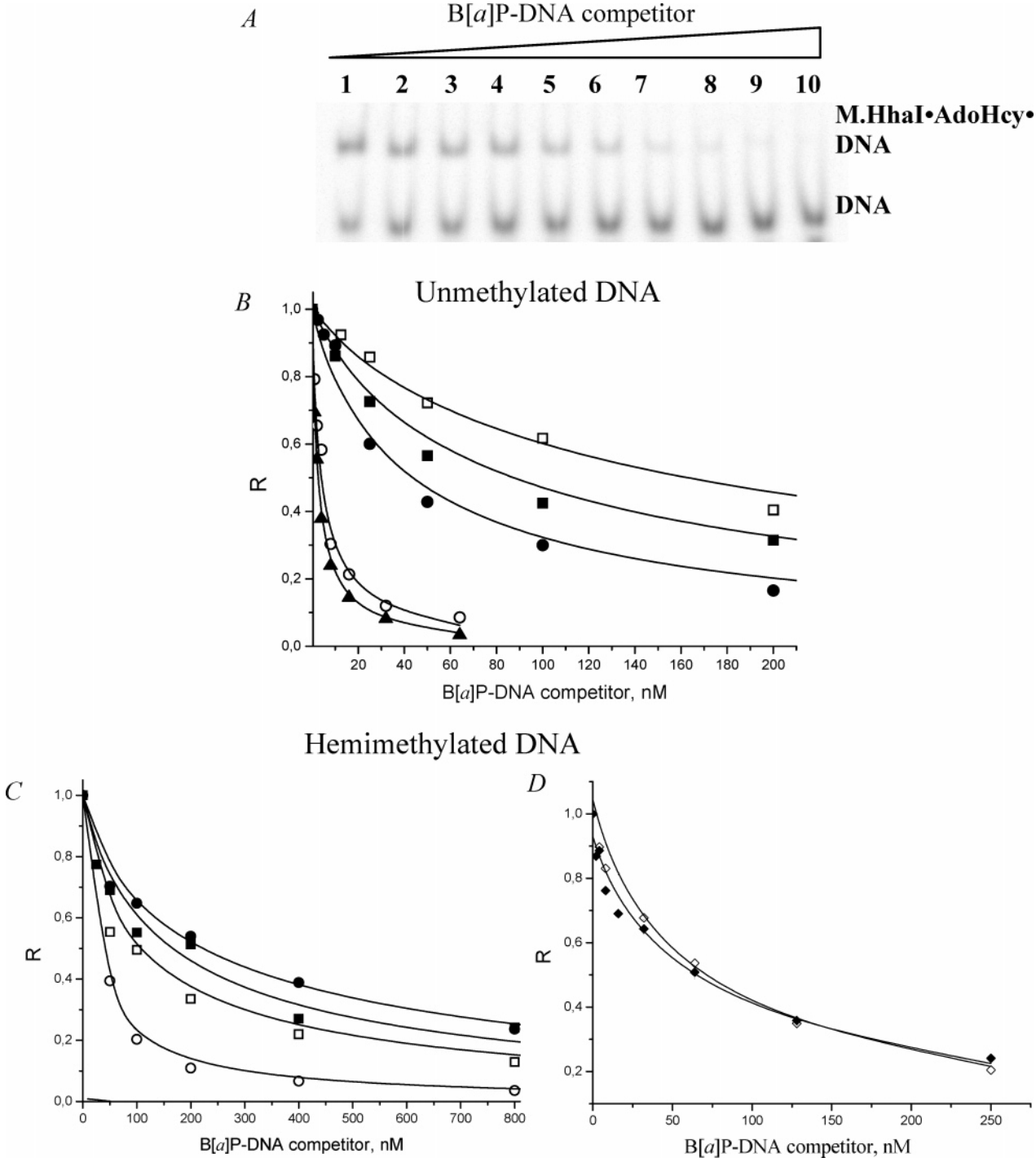

FIGURE 4: Competitive binding of B[*a*]PDE-modified oligodeoxynucleotide duplexes and unmodified oligodeoxynucleotide duplexes to M.HhaI. (A) Autoradiograph of EMSA of binding of unlabeled B[*a*]PDE-modified duplex B^+CG/CGM and ^{32}P-labeled unmodified duplex GCG/CGM to M.HhaI. GCG/CGM (2 nM) was mixed with increasing concentrations of competitor B^+CG/CGM (0, 0.05, 0.1, 0.2, 0.4, 0.8, 1.5, 3, 6, and 12 μM, numbered 1−10, respectively) and 1nM M.HhaI in buffer E containing 0.1 mM AdoHcy. (B, C, and D) Equilibrium competition curves for M.HhaI complexes with AdoHcy and ^{32}P-labeled duplex GCG/CGM in the presence of increasing concentrations of competitor B[*a*]PDE-modified duplexes. The definition of *R* and the designations of unmodified (GCG/CGC) and B[*a*]PDE-modified duplexes are as described in Figure 3.

and true equilibrium conditions may not have been achieved under our experimental conditions of relatively short incubation times. Therefore, in the case of M.HhaI, we used the apparent values $K_d^{r(app)}$ and K_d^{app}, where $K_d^{r(app)}$ and K_d^{app} are the *apparent* dissociation constants for unmodified (or reference) and B[*a*]PDE-modified duplexes, respectively. Because we were interested in the effects of the B[*a*]PDE residues on the binding of M.HhaI to DNA, we avoided the use of absolute K_d values and instead, defined the relative binding affinities, *k* (Table 3). In the case of the M.HhaI·B[*a*]P-DNA·AdoHcy complexes, the *k* values are equal to $K_d^{app}/K_d^{r(app)}$.

The K_d value of the ternary M.SssI·unmethylated B[*a*]P-DNA·AdoHcy complex (Table 2, duplexes BCG/CGC, GCB/CGC) is similar to the K_d value of the M.SssI·GCG/CGC·AdoHcy complex. Hence, the K_d values are independent of

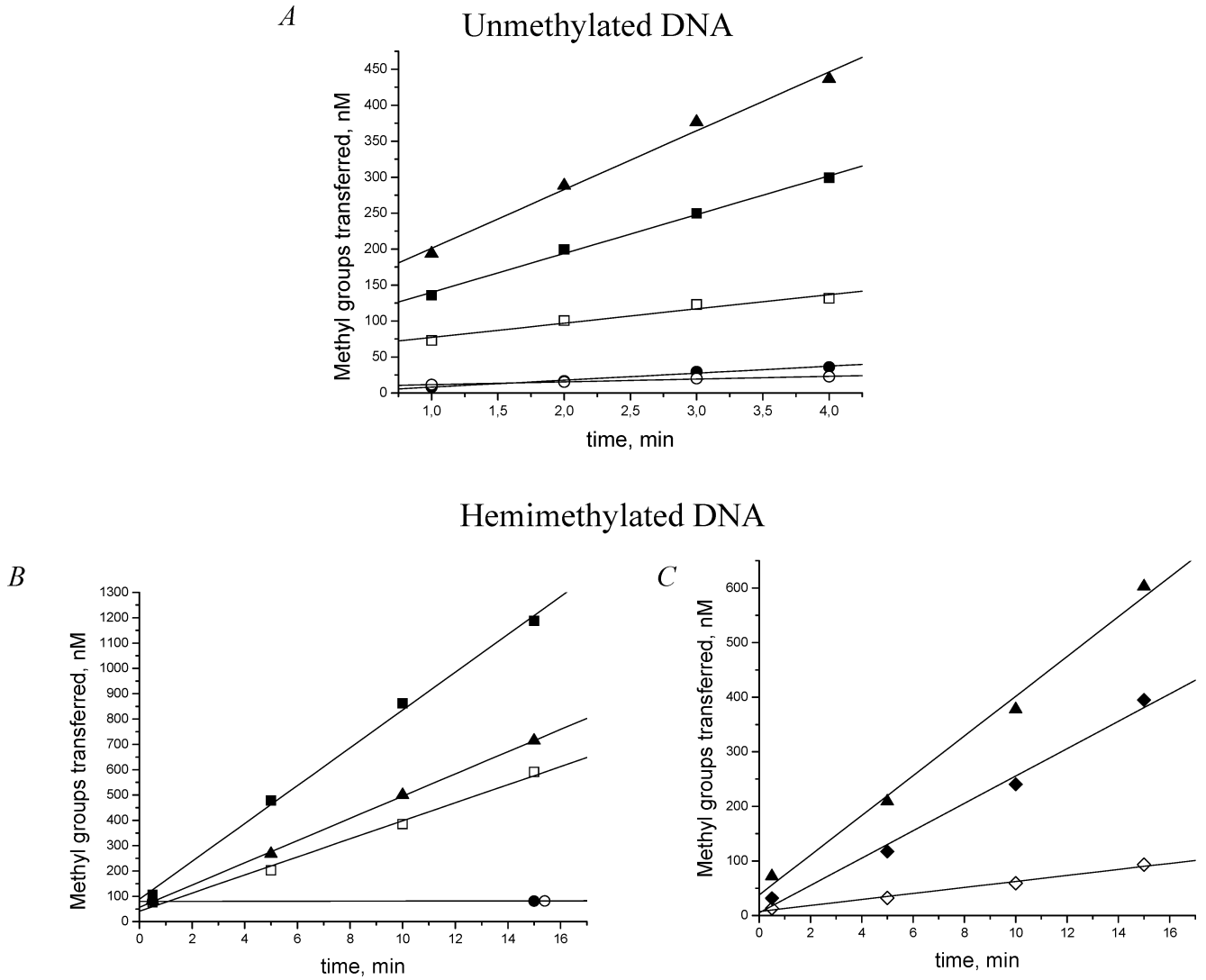

FIGURE 5: Steady-state kinetic analysis of the methylation of unmodified and B[*a*]PDE-modified unmethylated (A) and hemimethylated (B and C) oligodeoxynucleotide duplexes by M.SssI. The time dependences of ^{3}H-methyl group incorporation into B[*a*]P-DNA are at 37 °C. The reaction mixtures contained 1 μM DNA, 1.3 μM [CH_3-^{3}H]−AdoMet, and 18 nM M.SssI in buffer B. Unmodified duplexes GCG/CGC (A), GCG/CGM (B), and GMG/CGC (C) are designated by ▲. The designations of B[*a*]PDE-modified duplexes are as described in Figure 3.

the position of the B[*a*]P residues at BCG/CGC or GCB/CGC and the stereochemical characteristics of the (+)- or (−)-*trans*-adducts. The 5−9 nM range of the K_d values indicate that M.SssI forms tight complexes with the oligodeoxynucleotide duplexes with the B[*a*]P residues positioned either within the recognition sequence (GCB/CGC) or flanking this sequence on the 5′-side (BCG/CGC). Furthermore, M.SssI binds with high affinities to all hemimethylated duplexes containing B[*a*]P-N^2-dG adducts (BCG/CGM, GCB/CGM, and GMB/CGC) that are comparable to the affinities of the corresponding unmodified, parent duplexes GCG/CGM or GMG/CGC (Table 2). The largest effect was a 4.6-fold decrease in the binding affinity of the B^+CG/CGM duplex as compared to that of parent duplex GCG/CGM.

The bulky B[*a*]P residues clearly diminish the binding affinities of M.HhaI to the B[*a*]PDE-modified oligodeoxynucleotide duplexes (Table 3). The binding affinities of M.HhaI to the unmethylated B[*a*]PDE-modified duplexes BCG/CGC and GCB/CGC are reduced by factors of 3.3−45 relative to that of the unmodified GCG/CGC. The binding affinities of M.HhaI to the hemimethylated B[*a*]PDE-modified duplexes BCG/CGM, GCB/CGM, and GMB/CGC are reduced by factors of 17−100 in comparison with that for GCG/CGM. No distinct correlation was found between the binding affinity and adduct stereochemistry: in the case of duplexes BCG/CGC or BCG/CGM, M.HhaI binds less efficiently to the (+)-*trans*- than to the (−)-*trans*-adduct, whereas in the case of duplexes GCB/CGC, GCB/CGM, or GMB/CGC, M.HhaI binds more efficiently to the (+)-trans- than to the (−)-*trans*-adduct. In summary, the B[a]PDE lesions produce practically no effect on M.SssI binding to DNA and only moderately affect the binding of M.HhaI to DNA.

Steady-State Kinetics of Methylation of Stereoisomeric B[a]PDE-modified Oligodeoxynucleotide Duplexes by M.SssI and M.HhaI. The kinetics of methylation of duplexes GCG/CGC, BCG/CGC, GCB/CGC, GCG/CGM, BCG/CGM, GCB/CGM, GMG/CGC, and GMB/CGC by SssI and HhaI MTases was studied under steady-state conditions. The V_0 values for all oligodeoxynucleotide duplexes were determined from the initial linear portions of the product (methylated DNA) versus time profiles (Figures 5 and 6). The V_0 values

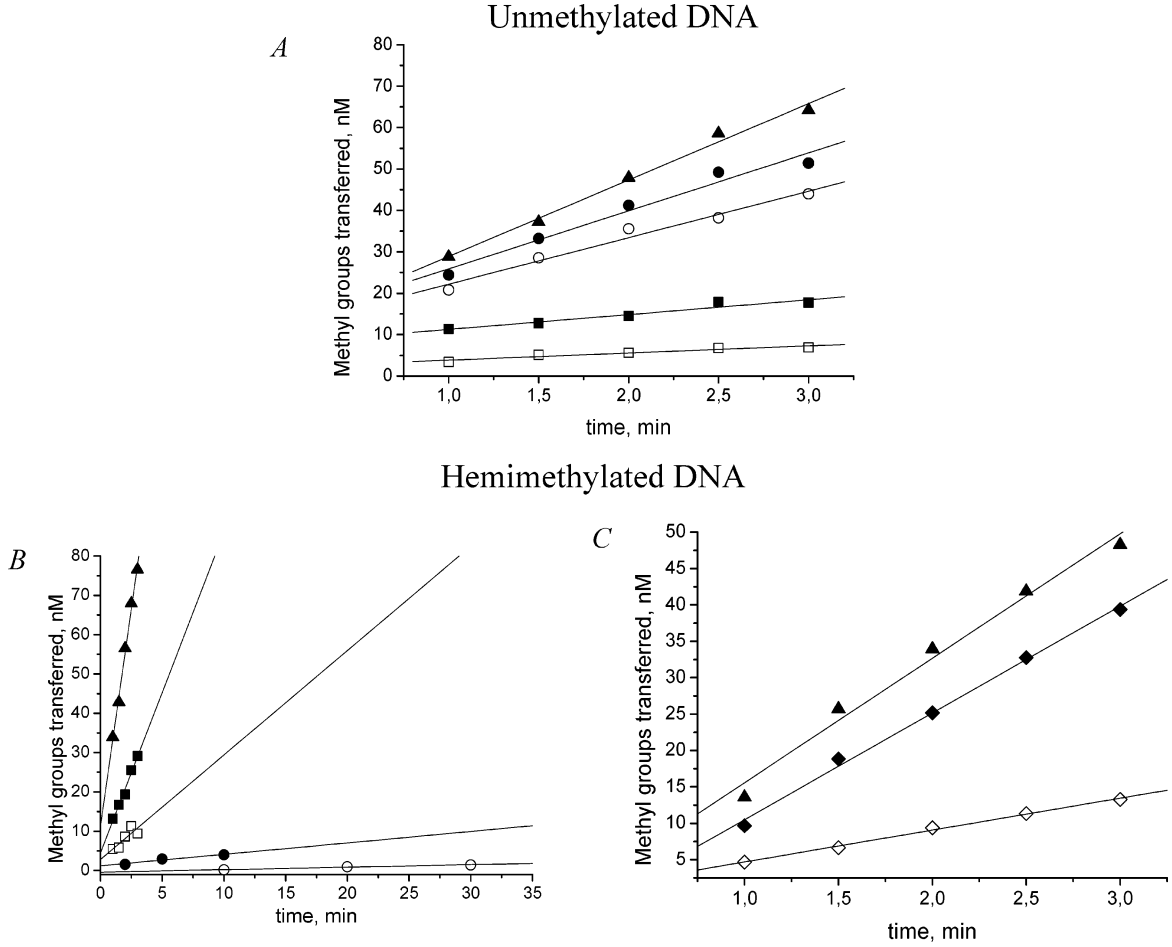

FIGURE 6: Steady-state kinetic analysis of the methylation of unmodified and B[*a*]PDE-modified unmethylated (A) and hemimethylated (B and C) oligodeoxynucleotide duplexes by M.HhaI. The time dependences of ^{3}H-methyl group incorporation into B[*a*]P-DNA are at 37 °C. The reaction mixtures contained 100 nM DNA, 1.3 μM [CH_3-^{3}H]−AdoMet, and 5 nM M.HhaI in buffer D. The designations of unmodified and B[*a*]PDE-modified duplexes are as described in Figure 5.

were determined at various substrate concentrations. In the case of both enzymes, the oligodeoxynucleotide duplex concentrations exceeded the K_d value of M.SssI·GCG/CGC·AdoHcy (Table 2) and K_d value of the M.HhaI·37-mer-DNA·AdoHcy (*44*) complexes by factors of 10^2-10^6. In the duplex concentration ranges tested, the measured V_0 values were independent of concentration for each unmodified or B[*a*]-PDE-modified duplex, thus indicating that the V_{max} limit was reached. Using the V_{max} values thus obtained, the k_{cat} values were calculated (Tables 2 and 3).

The methylation of the unmethylated B[*a*]PDE-modified duplexes (BCG/CGC and GCB/CGC) by both enzymes was moderately decreased, in comparison with that of parent duplex GCG/CGC, [1.3−4-fold in the case of M.HhaI (Table 3, Figure 6A) and 2−22-fold in the case of M.SssI (Table 2, Figure 5A)]. It is evident that M.HhaI transfers a methyl group to the B[a]PDE-damaged unmethylated duplexes BCG/CGC or GCB/CGC more efficiently than M.SssI. In the case of methylation reactions catalyzed by M.SssI, the presence of (+)- or (−)-*trans-anti*-B[*a*]P-N^2-dG adducts (B^+CG/CGC or B^-CG/CGC) flanking the target dC on the 5′-side resulted in a greater decrease in the k_{cat} value (9−22-fold) compared to the k_{cat} values for the replacement of dG that is 3′ adjacent to the target dC (GCB^+/CGC or GCB^-/CGC), which resulted in a decrease of k_{cat} values by a factor of 2−5. In the case of the M.HhaI reactions, when the adduct flanks the target dC residue on the 3′-side (GCB^+/CGC or GCB^-/CGC), the k_{cat} value decreases to a larger extent than in the case of the adduct flanking the same residue on the 5′-side. Among all unmethylated B[*a*]PDE-damaged oligodeoxynucleotide duplexes (Tables 2 and 3), the most significant effect on methylation (a 22-fold decrease) was observed in the case of M.SssI when the (−)-*trans-anti*-B[*a*]P-N^2-dG adduct flanked the target dC on the 5′-side (duplex B^-CG/CGC).

In contrast to unmethylated DNA, the methylation of the hemimethylated oligodeoxynucleotide duplexes BCG/CGM, GCB/CGM, and GMB/CGC by both M.SssI and M.HhaI reveals a much stronger dependence on the position of the adduct. The most striking effect on methylation rates was observed when one of the two stereoisomeric (+)- or (−)-*trans-anti*-B[*a*]P-N^2-dG adducts flanked the target residue on the 5′-side (BCG/CGM). It is noteworthy that in the case of M.SssI the modified G* residue in duplexes BCG/CGM is positioned outside of the recognition sequence. The methylation of these duplexes by M.SssI was completely abolished (Table 2, Figure 5B). The methylation of duplexes B^+CG/CGM and B^-CG/CGM by M.HhaI was dramatically decreased by a factor of 185 and 820, respectively, compared to that of parent duplex GCG/CGM (Table 3, Figure 6B). We also tested whether the inhibition of M.SssI and M.HhaI by the *trans-anti*-B[*a*]P-N^2-dG adducts in the BCGC nucleotide fragment was independent of the nucleotide adjacent to the *trans-anti*-B[*a*]P-N^2-dG residue on the 5′-side. We studied the effects of dT or dA flanking the B[a]P-N^2-dG

adduct on the 5′-side on methylation using the hemimethylated oligodeoxynucleotide duplexes 5′-GAGCCAAGMG-CACTCTGA/5′-TCAGAGTBCGCTTGGCTC. In these duplexes, the nucleotide 5′ adjacent to B^+ or B^- was dT instead of dA, as it is in the case of duplexes BCG/CGM. The methylation of duplexes 5′-GAGCCAAGMGCACTCTGA/5′-TCAGAGTBCGCTTGGCTC was completely abolished in the case of M.SssI or dramatically reduced in the case of M.HhaI (data not shown). Therefore, the inhibition of methylation is independent of the nucleotide flanking the *trans-anti*-B[*a*]P-N^2-dG lesions in the BCGC nucleotide fragment on the 5′-side. When the B[*a*]P-N^2-dG adduct was 3′ adjacent to the target dC (duplexes GCB/CGM), we observed a 1.2−8-fold decrease of methylation by both MTases. Only in the case of duplex GCB^+/CGM, the methylation by M.SssI was increased by a factor of 1.6 (Table 2, Figure 5A). With the *trans-anti*-B[*a*]P-N^2-dG residues flanking m^5dC on the 3′-side (duplexes GMB/CGC), a small decrease in methylation rates (1.3−6-fold) was observed in the case of both MTases compared to that of parent duplex GMG/CGC. The methylation of either unmethylated (BCG/CGC and GCB/CGC) or hemimethylated (BCG/CGM, GCB/CGM, and GMB/CGC) duplexes was found to depend on adduct stereochemistry. In the case of both enzymes, the values of k_{cat} for (+) and (−)-isomers differ by factors of 1.2−4.7 (Tables 2 and 3). In all substrates, the methylation catalyzed by either M.SssI or M.HhaI is more efficient in duplexes with the (+)-*trans-anti*-B[*a*]P-N^2-dG lesions than with the (−)-*trans-anti*-B[*a*]P-N^2-dG adducts. In summary, under steady-state conditions, in most cases, the lesions either decrease the k_{cat} values or block methylation altogether in catalysis by either M.SssI or M.HhaI. The greatest impact of the B[*a*]P-N^2-dG lesions on methylation is observed when the lesion flanks the target dC residue on the 5′-side.

Single Turnover Kinetic Analysis of Methylation of Hemimethylated B[a]PDE-Modified Oligodeoxynucleotide Duplexes by M.SssI and M.HhaI. A study of methylation was conducted (*43*−*45*, *58*) under single turnover conditions aimed to determine the methylation rate constant (k_{chem}), which characterizes the chemical step of the methylation reaction. Recently, the relative contributions of various steps in the catalytic cycle of M.HhaI to k_{cat} were evaluated in a quantitative manner (*43*−*45*, *58*). It was demonstrated that product release ($k_{off} = 0.045\ s^{-1}$) was substantially slower than the preceding chemical step ($k_{chem} = 0.26\ s^{-1}$) and was the major contributor to the multiple turnover rate ($k_{cat} = 0.04\ s^{-1}$) of M.HhaI (*44*). The ratio k_{chem}/k_{cat} for methylation of a hemimethylated 30-mer and 37-mer oligodeoxynucleotide duplexes by M.HhaI varied from 3 (*43*) to 6−8 (*44*), respectively. In accordance with these data, the ratio k_{chem}/k_{cat} that we obtained for the 18-mer duplex GCG/CGM is ∼5 (Table 3).

The B[*a*]PDE-induced damage of DNA resulted in the reduction of the k_{chem} values for methylation of the hemimethylated B[*a*]P-N^2-dG adduct-containing duplexes BCG/CGM, GCB/CGM, and GMB/CGC catalyzed by M.SssI and M.HhaI, in comparison with that of hemimethylated duplex GCG/CGM (Figure 7, Tables 2 and 3). As in the steady-state kinetic experiments, the methylation under single turnover conditions was dependent on the adduct position and adduct stereochemistry. We did not observe any detectable level of (CH_3-^{3}H) incorporation into duplexes BCG/CGM by M.SssI after a 15 min incubation time. Only after a 2 h incubation period were we able to detect 5−8% methylation levels in the case of the (+)- and (−)-adducts relative to that for the same reaction with parent duplex GCG/CGM (data not shown). Methylation of duplexes BCG/CGM by M.HhaI resulted in a 410 or 2100 fold decrease in k_{chem} for the (+)- and (−)-adducts, respectively (Table 3). MTases SssI and HhaI transfer a methyl group to hemimethylated duplexes GCB/CGM and GMB/CGC with 1.3−20-fold slower rates than to the parent duplex GCG/CGM (Tables 2 and 3). As under steady-state conditions, M.SssI and M.HhaI methylate oligodeoxynucleotide duplexes containing the (+)-*trans-anti*-B[*a*]P-N^2-dG lesion more efficiently than those duplexes containing the (−)-stereoisomeric lesion (Tables 2 and 3).

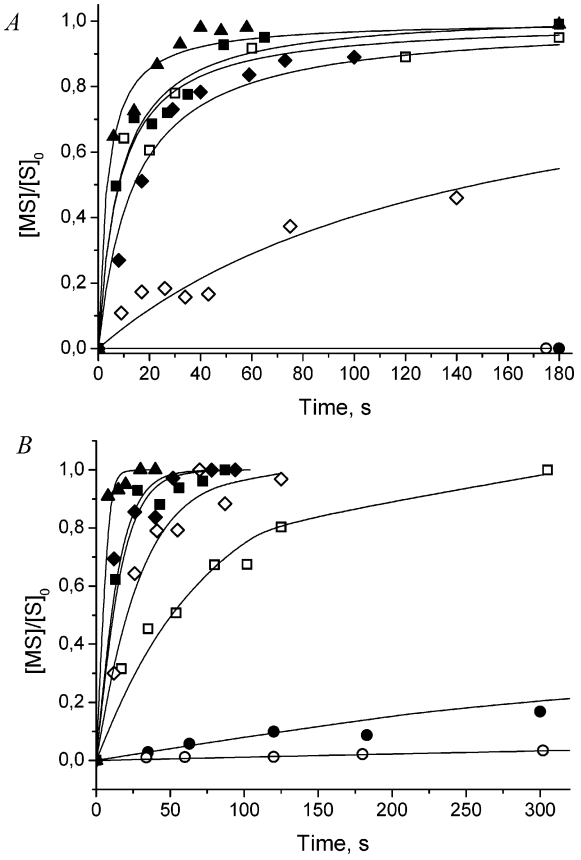

FIGURE 7: Single turnover kinetic analysis of methylation of hemimethylated oligodeoxynucleotide duplexes by M.SssI (A) or M.HhaI (B). The time dependence of ^{3}H-methylated product concentration ([MS]) is normalized to the total DNA concentration ([S]$_0$). The reaction mixtures contained 100 nM DNA, 1.3 μM [CH_3-^{3}H]−AdoMet and 1.3 μM M.SssI or 1.0 μM M.HhaI in buffers B or D, respectively. The designations of unmodified and B[*a*]PDE-modified duplexes are as described in Figure 3 (C and D).

In summarizing the results on the impact of the B[*a*]P-N^2-dG adducts on various steps in the methylation catalytic cycle, we concluded that these lesions decrease the multiple turnover and single turnover rates of a methyl transfer.

DISCUSSION

In this study, the impact of the *trans-anti*-B[*a*]P-N^2-dG adducts positioned within CpG and GCGC sequences in double-stranded DNA on the functional properties of two prokaryotic MTases, namely SssI and HhaI, has been

examined. It is useful to consider the structural characteristics of the B[*a*]P-DNA adducts and complexes of C5 MTases with their unmodified DNA substrates. Solution NMR studies have shown that the bulky aromatic B[a]P ring systems of the (+) and (−)-*trans-anti*-B[a]P-N^2-dG adducts reside in the minor groove of the double helix pointing toward the 5′- or 3′-directions of the modified strands, respectively (*59*−*63*). The Watson−Crick base pairing was found to be intact at the lesions site as well as at all base pairs flanking the *trans-anti*-B[*a*]P-N^2-dG adducts in a CBC sequence context (60) as in duplexes GCB/CGC and GCB/CGM.

The primary structure of M.HhaI, as is typical of other bacterial C5 MTases, consists of 10 conserved motifs that include residues responsible for AdoMet binding and the catalysis of the methyl transfer reaction (*6*, *40*). From cocrystal structures of complexes of M.HhaI with DNA and AdoMet or AdoHcy, it is known that M.HhaI folds in two domains (*40*, *41*). The large domain encompasses the AdoMet binding site and the catalytic center, whereas the small domain contains the target recognition domain. The methylation of the cytosine does not take place when this residue is in its normal position within the double helix. Instead, the target cytosine residue flips out of the DNA double helix and inserts itself into the active site pocket of M.HhaI (*40*, *41*). The flipping out of the target cytosine is accompanied by a motion of the catalytic loop of M.HhaI toward the minor groove side of the DNA substrate.

The MTase SssI recognizes CpG sequences and is highly homologous with all of the conserved regions of M.HhaI and other prokaryotic C5 MTases (*37*, *39*). A theoretical model of a ternary M.SssI·DNA·AdoHcy complex was recently constructed using previously solved crystal structures of M.HhaI and M.HaeIII as templates (*39*). According to this model, M.SssI is predicted to have a bi-lobal structure with the cofactor binding and catalytic sites located in the large domain, whereas the target recognition domain is located in the small domain. However, the M.SssI·DNA interface differs from that of the M.HhaI·DNA complex (*39*, *41*, *54*). According to the model (*39*) and the footprint analysis of M.SssI (*54*), one can suggest that there are fewer contacts between M.SssI and the nucleobases of the recognition sequence than in the case of M.HhaI, but there are more contacts with phosphate groups, including those of the flanking nucleotide sequences.

The presence of the B[*a*]PDE residues in the modified dG exerts different effects on the binding of the DNA substrates by MTases SssI and HhaI. In the case of M.SssI, which recognizes CpG sequences, the lesions have virtually no effect on the binding affinity of M.SssI to DNA, regardless of the position of the adduct, its stereochemistry, and the presence of m^5dC rather than the target dC residues (Table 2). According to the model of the M.SssI·DNA·AdoHcy complex, most of the sequence-specific DNA−protein contacts are located within the major groove of the double helix (*39*). Accordingly, the introduction of the B[*a*]PDE residue into the DNA minor groove does not perturb the sequence-specific recognition of DNA by M.SssI.

In the case of M.HhaI, in contrast to the case of M.SssI, the affinity of binding of the MTase to B[*a*]PDE-modified duplexes was 1 to 2 orders of magnitude smaller than that to the parent duplexes (Table 3). This finding can be considered in the light of the known mechanism of action of M.HhaI. The interaction of M.HhaI with DNA includes several consecutive steps: the formation of the enzyme·DNA·AdoMet complex, the flipping of the target dC out of the double helix, a catalytic loop locking, the covalent bonding between MTase and DNA, the methyl transfer, and the dissociation of the reaction end products (*40*, *43*, *44*, *58*). The double-stranded DNA substrate fits into the cleft between the two domains of M.HhaI with the major groove facing the small domain and the minor groove facing the large domain (*41*). Most of the M.HhaI−DNA contacts formed, which constitute the recognition step of DNA by M.HhaI (base-specific interactions), occur via the two recognition loops from the small domain of the enzyme and the major groove of DNA (*41*). Because the B[*a*]PDE residue is located in the minor groove, it can be argued that the observed increase in the K_d^{app} values is not due to a perturbation of the base-specific interactions. It was shown that the target cytosine flipping occurs most likely through the major groove of the DNA duplex (*42*). The flipped out cytosine is held in place by contacts with the amino acids from the catalytic loop (Phe^{79} and Cys^{81}) and by the other amino acids (Glu^{119}, Val^{121}, and Arg^{165}) of the large domain of M.HhaI (*41*). It is known that the $Val^{121} \rightarrow$ Ala mutant of M.HhaI, a mutation that interferes with the stabilization of the target cytosine, exhibits a 10^5-fold decrease in K_d (*58*). From the other side, the stability of the activated target base depends on MTase catalytic loop locking, which is dependent on the contacts of Ser^{85}, Ile^{86}, Lys^{89}, and Arg^{97} (all in the catalytic loop) with the DNA minor groove (*41*, *64*). The observed reduction of the binding of M.HhaI to the B[*a*]-PDE-modified oligodeoxynucleotide duplex may be explained by a perturbation of the contacts of the catalytic loop of M.HhaI with the minor groove of the DNA double helix that normally help to stabilize the catalytic loop.

The interaction of M.EcoRII with the oligodeoxynucleotide duplexes containing *trans-anti*-B[*a*]P-N^2-dG adducts within the CC(T/A)GG recognition sequence also resulted, as in the case of M.HhaI, in a 5−30-fold decrease in the binding affinity of the enzyme to DNA (*32*). It appears that M.HhaI and M.EcoRII (and probably other prokaryotic MTases that recognize 4−8 base pair sequences in DNA) are more sensitive to the alterations of nucleobases within the recognition sequence than the CpG-recognizing M.SssI. Accordingly, the binding of M.SssI to oligodeoxynucleotide duplexes containing a C·A mismatch in place of a C·G base pair within the recognition sequence was conserved, whereas the binding of M.HhaI to this oligodeoxynucleotide duplex was abolished (*65*).

In contrast to the observed changes in binding, we observed basically analogous effects of the B[a]P-N^2-dG adducts on methylation rates catalyzed by the SssI and HhaI MTases (Tables 2 and 3). These observations may be related to the similar catalytic mechanisms observed with different C5 MTases (*35*, *36*). In most cases, B[*a*]P-N^2-dG adducts decreased the methylation of hemimethylated and unmethylated substrates. The effects of these lesions on the methylation of the hemimethylated oligodeoxynucleotide duplexes (BCG/CGM, GCB/CGM, and GMB/CGC) catalyzed by both MTases are stronger than on the methylation of the unmethylated duplexes (BCG/CGC and GCB/CGC). Importantly, under steady state as well as single turnover conditions, in the case of the hemimethylated duplexes, the *trans-*

anti-B[*a*]P-N^2-dG adduct greatly diminishes the methylation efficiency of the dC target residue (underlined in Tables 2 and 3) when it is positioned on its 5′-side, but the impact is relatively minor when the *trans-anti*-B[*a*]P-N^2-dG adduct is positioned on its 3′-side in the same strand. In GMB/CGC duplexes, when the target dC residue is positioned in the unmodified strand opposite to the B[*a*]PDE-modified dG residue, the effect on k_{cat} is relatively small (compared to that of duplexes BCG/CGM) and is diminished by factors of only 1.5−6 (GMB/CGC, Tables 2 and 3).

Before considering the positional effects in more detail, we considered the effects of adduct stereochemistry on the impairment of the methylation of the B[*a*]PDE-modified duplexes by M.HhaI and M.SssI. Although the methylation efficiencies are more dependent on the position of the adduct relative to that of target C than on the stereochemical properties of the (+)- and (−)-*trans-anti*-B[*a*]P-N^2-dG adducts, the rates are somewhat smaller for the (−)-trans-adducts than the (+)-trans-adducts in all duplexes in the case of M.SssI (Table 2), and in BCG/CGM, GCB/CGM, and GMB/CGC duplexes in the case of M.HhaI (Table 3). Particularly informative are the experiments with the hemimethylated sequences BCG/CGM, GCB/CGM, and GMB/CGC because each of these duplexes has only one target dC residue (underlined in Tables 2 and 3) rather than two such residues in duplexes BCG/CGC and GCB/CGC. The dramatic adverse impact of the adducts on k_{cat} is observed when the target dC is flanked by either the B^+ or B^- adducts on its 5′-side.

In the case of B[*a*]PDE-modified duplexes BCG/CGC, GCB/CGC, BCG/CGM, GCB/CGM, and GMB^+/CGC, the somewhat greater adverse impact of the (−)-*trans-anti*-B[*a*]P-N^2-dG adducts than the (+)-*trans-anti*-B[*a*]P-N^2-dG adducts may be related to their known structural characteristics and conformations in DNA (*59*), assuming that the latter remain relatively undistorted in the DNA−protein complexes. In these adducts, the bulky pyrenyl residues are located in the minor groove, pointing to either the 5′ or the 3′ directions of the modified strands in the case of the (+)-*trans*- and (−)-*trans*-adducts, respectively, whereas the saturated 7,8,9,10 rings protrude into the 3′ direction ((+)-*trans*-adduct) and into the (5′ direction ((−)-*trans*-adduct)). A more detailed structural analysis reveals that because of the helical twist the (+)-adduct is less easily accommodated in the minor groove than the (−)-adduct (*66*). This results in a greater widening of the minor groove and a greater solvent exposure of the pyrenyl residue in the (+)-*trans* than in the (−)-*trans*-adduct. These conclusions (*66*) are in agreement with experimental thermodynamic measurements of solvent exposure (*67*) and the pronounced greater extent of bending of the DNA duplex with (+)-*trans-anti*-B[*a*]P-N^2-dG adducts than with (−)-*trans-anti*-B[*a*]P-N^2-dG adducts in CBC sequence contexts (*63*, *68*). These bulky B[a]PDE residues may, in general, interfere with the rearrangement of the catalytic loop and prevent the formation of important minor groove DNA−enzyme contacts that stabilize the catalytic loops and the target cytosine residues. However, the stereoisomeric effects on k_{cat} seem to be better correlated with the overall greater structural distortions and bending associated with the (+)-*trans*-adduct. These distortions may result in a greater structural local flexibility in the case of the (+)-*trans*- than the (−)-*trans*-adduct (*63*, *68*), which might favor the formation of protein−DNA conformations that favor the methylation process in the B^+CG/CGC, GCB^+/CGC, B^+CG/CGM, GCB^+/CGM, and GMB^+/CGC duplexes catalyzed by M.HhaI and M.SssI. In the case of duplex GMB^-/CGC, where m^5dC is 5′ to the (−)-*trans-anti*-B[*a*]P-N^2-dG adduct, an intercalative B[*a*]P alignment with a concomitant displacement of the modified guanine and the partner cytosine residues into the minor and major grooves, respectively, has been found (*69*, *70*). Such intercalative B[*a*]P alignment in duplex GMB^-/CGC does not seem to have a strong effect on its methylation, even though the target dC residue is already flipped out of the duplex, even in the absence of the protein.

To account for the positional effects of the B[*a*]PDE lesions on differences in the methylation rates of hemimethylated duplexes BCG/CGM, GCB/CGM, and GMB/CGC by M.HhaI, we took advantage of the known ternary structure of the M.HhaI·DNA·AdoHcy complex, where the target cytosine is already flipped out (*71*). Figure 8Ademonstrates that the amino acids in the catalytic loop of M.HhaI (Phe^{79}, Cys^{81}, Ser^{85}, Ile^{86}, Lys^{89}, and Arg^{97}) and in the target recognition domain (Gln^{237}) form contacts with the DNA from the minor groove side (*71*). The peptide backbone of Ile^{86} in the catalytic loop forms a hydrogen bond with the exocyclic amino group of the guanine residue 5′ to the target cytosine. The catalytic loop stabilizes the flipped out cytosine, the process being dependent on this hydrogen bond (*64*). We speculate that in the case of the B[*a*]PDE-modified duplexes B^+CG/CGM and B^-CG/CGM that were characterized by strongly reduced methylation rates, the bulky B[*a*]P-N^2-dG adducts on the 5′-side of the target dC residue abolish the important DNA−enzyme contacts that stabilize the catalytic loop of M.HhaI, primarily contacts of Ile^{86} with the amino group of the B^+ or B^- adducts. Figure 8B schematically represents how B[*a*]P-N^2-dG might be accommodated in the structure of the original M.HhaI·DNA·AdoHcy complex. We took as an example duplex B^+CG/CGM with the (+)-*trans-anti*-B[*a*]P-N^2-dG adduct positioned on the 5′-side of the target dC. It is evident that the bulky B[a]P residue that resides in the minor groove may disturb the contacts of the individual amino acids of the catalytic loop with the DNA.

In the case of duplexes GCB/CGM, where the *trans-anti*-B[*a*]P-N^2-dG adducts are positioned on the 3′-side of the target dC residue, the methylation efficiency is retained. These results suggest that most of the critical DNA−enzyme contacts on the minor groove side (Figure 8A) are not perturbed in this complex.

According to X-ray data, the O6, N1, and N^2 atoms of the dG residue that are partnered with the target dC residue are in contact with Gln^{237} in the target recognition domain (*40*, *41*, *71*) (Figure 8). Amino acid Gln^{237} plays a key role in the flipping of the target dC residue out of the oligodeoxynucleotide duplex (*45*). Perturbation of the contacts of Gln^{237} with the dG residue paired with the target dC results in a dramatic impairment of base flipping although the stability of the specific binding of the DNA to the enzyme is retained (*45*). In duplexes GMB^+/CGC and GMB^-/CGC, the B[*a*]P residue is covalently attached to the guanine of the G·C base pair that contains the target dC residue. Because the methylation of duplex GMB^+/CGC and, presumably, the base flipping activity was practically unchanged by the

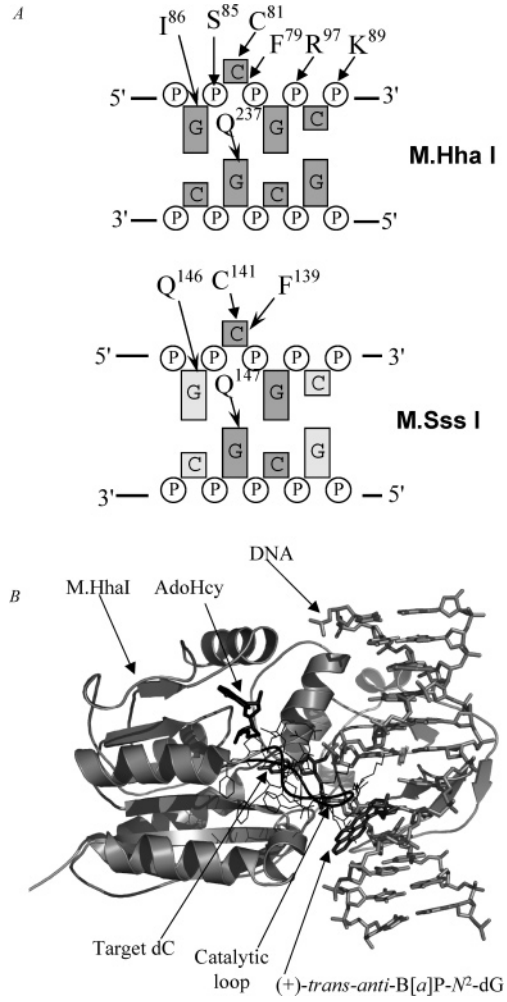

FIGURE 8: (A) Schematic diagrams showing the contacts of M.HhaI and M.SssI with DNA from the minor groove side. The nucleoside residues are represented by rectangles and backbone phosphates are represented by circles. Interacting protein residues are represented by their single-letter identifiers and numbers. HhaI and SssI sites are shown in dark gray. These schemes were derived from the crystal structure of the M.HhaI·DNA·AdoHcy complex (*71*) and a model of the M.SssI·DNA·AdoHcy complex (*39*). (B) Model illustrating the possible accommodation of the (+)-*trans-anti*-B[*a*]P-N^2-dG into the structure of the M.HhaI·DNA·AdoHcy complex (*71*). The 3D structure of the ternary complex of M.HhaI with the 12-mer oligodeoxynucleotide duplex containing GCGC, and the cofactor analogue AdoHcy was from the RCSB Protein Data Bank. The (+)-*trans-anti*-B[*a*]P-N^2-dG was created using ACD/ChemScetch and then introduced into the position 5′ adjacent to the target dC (as in duplex B^+CG/CGM) of the 12-mer duplex using ACD/3D Viewer and PyMOL v0.98. According to refs *59* and *60*, the B[a]P residue of the (+)-*trans-anti*-B[*a*]P-N^2-dG adduct was put into the minor groove of the double helix pointing toward the 5′ direction of the modified strand. The catalytic loop, the flipped out cytosine, AdoHcy, and the B[*a*]P are in black. The enzyme is shown in ribbon representation. The amino acids of the catalytic loop are shown both in ribbon and wireframe representation. DNA and AdoHcy are shown in the stick representation.

adduct, we assumed that the contacts of the modified dG residue with Gln^{237}, in this case, were intact. A slight reduction of the methylation rate constant of duplex GMB^-/CGC can be explained by the violation of some contacts of the modified dG residue with Gln^{237} due to the displacements of the modified dG and the target dC residues into the minor and the major grooves, respectively, with the B^- adduct positioned in the GMB^-C context (*69*, *70*).

To account for the position-dependent effect of the B[*a*]P-N^2-dG adduct on the methylation of hemimethylated duplexes BCG/CGM, GCB/CGM, and GMB/CGC by M.SssI, we made use of the available model of the ternary M.SssI·DNA·AdoHcy complex (*39*). Such comparisons are facilitated because the 5′-CCAAGCGCACTC/5′-GAGTGCGCTTGG duplex used in this modeling study is the same as the central sequence context of duplex GCG/CGC (Table 2). Taking into account the similarities in the structures of HhaI and SssI MTases (*39*), and on the basis of similar catalytic mechanisms of C5 MTases (*35*, *36*), we propose here that M.SssI, like M.HhaI (*41*), flips the target dC residue out of the duplex, which is accompanied by a movement of the catalytic loop toward the DNA molecule. According to this model, amino acid residues Phe^{139}, Cys^{141}, Gln^{146}, and Gln^{147} in the catalytic loop of M.SssI form contacts with the DNA from the minor groove side (*39*) (Figure 8A). When *trans-anti*-B[*a*]P-N^2-dG flanks the target dC on the 5′-side in duplex BCG/CGM, methyl transfer is blocked. In this case, the bulky polycyclic aromatic ring system of the adduct may perturb the flipping of the target cytosine out of the helix and/or the rearrangement of the catalytic loop. Because methylation is essentially inhibited, even under single turnover conditions for 2 h, one may assume that the flipping of the target base is impeded. Therefore, the presence of *trans-anti*-B[*a*]P-N^2-dG 5′ adjacent to the CpG dinucleotide (BCG) is especially unfavorable for cytosine methylation in this CpG sequence.

In contrast, when the B[*a*]P-N^2-dG adduct is positioned adjacent to the target dC residue on the 3′-side in the CpG sequence (GCB/CGM), no decrease in methylation was observed. According to the model of the M.SssI·DNA·AdoHcy complex, M.SssI interacts with this dG residue from the major groove side and does not have any contacts with the protein on the minor groove side (*39*). Therefore, the formation of the M.SssI·DNA·AdoHcy complex is not affected by the B[*a*]P-N^2-dG adduct in the GCB sequence context. In the case of GMB/CGC duplexes, the B[*a*]P residue may perturb the contact of Gln^{147} with the exocyclic amino group of the *trans-anti*-B[*a*]P-N^2-dG adduct that is paired with the target dC residue (*39*) (Figure 8A). Indeed, the k_{cat} values for GMB/CGC duplexes are smaller than that in the case of parent duplex GMG/CGC. This accounts for the greater impact of the B[*a*]P residue on methylation when the *trans-anti*-B[*a*]P-N^2-dG lesion is located opposite the target dC, rather than adjacent to it on the 3′-side. Because both duplexes GCB/CGM and GMB/CGC are methylated by M.SssI, we speculate that the target dC residue can be successfully flipped out of the helix in these M.SssI·DNA complexes.

There may exist alternative explanations of the effects of B[*a*]P-DNA adducts on methylation due to the hypothetical possibility that MTases can bind to the hemimethylated duplexes in two orientations when the active site is oriented toward the target cytosine or toward the methylated cytosine. In the case of the hemimethylated B[*a*]PDE-modified duplexes (e.g., in the case of duplex BCG/CGM), this means that an MTase could bind to DNA in orientation #1 or in orientation #2 (Figure 9). If an MTase is able to bind to B[*a*]P-DNA in orientation #2, the methylation reaction cannot take place because this orientation is nonproductive. It is known that M.HhaI binds unmodified hemimethylated

#1 (active site side)	#2 (active site side)
BCGC	GMGC
CGMG	CGCB

FIGURE 9: Strand selectivity upon binding of M.SssI or M.HhaI to duplex B^-CG/CGM (or B^+CG/CGM). The target cytosine (C) or the 5-methylcytosine (M) obtained after methylation of the target cytosine are underlined.

target sites in the productive orientation (when the active site is oriented toward the target cytosine) with high selectivity (*44*). This suggests that M.HhaI binding to B[*a*]-PDE-modified oligodeoxynucleotide duplexes in the nonproductive orientation #2 is unlikely. The question whether M.SssI is able to distinguish between unmethylated and methylated strands of the unmodified hemimethylated duplex is not resolved. Our kinetic data indicate that unmethylated oligodeoxynucleotide duplex GCG/CGC is two times more efficiently methylated by M.SssI than hemimethylated duplexes GMG/CGC or GCG/CGM. This could be indirect evidence that M.SssI could bind hemimethylated target sites in two orientations, and in essence, the nonproductive orientation (when the active site is oriented toward the 5-methylcytosine) could serve as a competitive inhibitor for the productive orientation. If introduction of the B[*a*]P residue into the hemimethylated duplex results in the increase of the amount of nonproductive orientation # 2, then binding of M.SssI to duplex BCG/CGM in nonproductive orientation #2 may contribute to the lack of methylation observed in this case (Table 2).

Guanine residues in DNA are often the most common sites not only of B[*a*]PDE DNA damage but also of oxidative and alkylation DNA damage (*72*−*74*). The replacement of the 3′-flanking guanine residue adjacent to the target cytosine in the hemimethylated CpG sequence context by 8-hydroxyguanine (*75*) or by O^6-methylguanine (*76*) resulted in the inhibition of DNA methylation by the eukaryotic MTase Dnmt1. When 8-hydroxyguanine (*75*) or O^6-methylguanine (*76*, *77*) are positioned opposite to the target cytosine in the hemimethylated CpG sequence context, the methylation of the target cytosine by Dnmt1 is not altered and can be even enhanced. Thus, there are similarities in the effects of oxidative, alkylation, and B[*a*]PDE modifications of the dG residue opposite to the target dC on DNA methylation. However, a B[*a*]P-N^2-dG adduct flanking the target dC on its 3′-side does not exert as dramatic an effect on CpG methylation as that of oxidative and alkylation damage to the same dG residue.

On the basis of similarities in the catalytic mechanisms observed with mammalian and prokaryotic MTases (*35*, *36*), similar phenomena to those observed here may be relevant in eukaryotic cells as well. In living cells, unrepaired B[*a*]P-DNA adducts are found in significant quantities (*78*−*80*), and the hot spots of such damage are located in CpG-rich regions (*81*, *82*). In addition to the effects of B[*a*]P-N^2-dG adducts on DNA sequence mutations, some *trans-anti*-B[*a*]P-N^2-dG adducts that escape repair may also give rise to a hypomethylation effect of the B[*a*]PDE-damaged DNA. Earlier, it was observed that the treatment of eukaryotic cells with benzo[*a*]pyrene has generally resulted in a decrease in the genomic 5-methylcytosine levels (*30*, *83*). According to our results, the site-specific introduction of the *trans-anti*-B[*a*]P-N^2-dG adducts into DNA can lead to a local hypomethylation, this effect being dependent on the position of the lesion. The adducts in eukaryotic cells may affect de novo methylation (*6*, *7*, *84*) and may be located either in unmethylated DNA or in hemimethylated DNA formed after the first step of de novo methylation. A strongly reduced rate or complete block of B[*a*]P-DNA methylation may result in an altered methylation pattern. As for maintenance methylation, the influence of hemimethylated duplexes containing (+) or (−)-*trans-anti*-B[*a*]P-N^2-dG adducts on the 5′- or 3′-sides of the target dC on the methylation status is unlikely because the probability of formation of these duplexes after DNA replication, but before DNA methylation, is small. However, duplex GMB^-/CGC containing m^5dC adjacent to the (−)-*trans-anti*-B[*a*]P-N^2-dG adduct on its 5′-side could arise after DNA replication with high probability (*25*−*27*), and thus could affect maintenance methylation. The methylation of duplex GMB^-/CGC occurs with a reduced rate (Tables 2 and 3). However, the (−)-*trans* isomer of B[*a*]-PDE is not formed to any significant extents in eukaryotic cells (*85*).

Further studies of the interactions of mammalian MTases with site-specific B[*a*]P-N^2-dG adducts in DNA should provide new information on the impact of these lesions on DNA methylation in eukaryotic cells.

ACKNOWLEDGMENT

We thank Dr. B. Jack and Dr. G. Wilson from New England Biolabs for their generous gift of the M.SssI plasmid, Dr. S. Klimasauskas for his generous gift of M.HhaI, Dr. S. A. Eremin for assistance in fluorescence polarization experiments, Dr. O. V. Petrauskene and Dr. V. N. Tashlitsky for the discussion of the problem of the impact of DNA damage on DNA methylation, and Dr. A. V. Golovin for help in constructing the model of the M.HhaI•B[*a*]P-DNA complex.

SUPPORTING INFORMATION AVAILABLE

The T_m values for oligodeoxynucleotide duplexes GCG/CGC, B^+CG/CGC, B^-CG/CGC, GCB^+/CGC, GCB^-/CGC, GCG/CGM, B^+CG/CGM, B^-CG/CGM, GCB^+/CGM, GCB^-/CGM, GMB^+/CGC, and GMB^-/CGC, the derivation of equation for quantitative treatment of equilibrium competition experiments, the determination of the amount of the active form of M.SssI by equilibrium competitive binding, the kinetic analysis of formation of complex of M.SssI and M.HhaI with DNA in competitive binding, and the representative data for the determination of the dissociation rate constant for the binding of M.SssI to GCG/CGM are presented. This material is available free of charge via the Internet at http://pubs.acs.org.

REFERENCES

1. Momparler, R. L., and Bovenzi, V. (2000) DNA methylation and cancer, *J. Cell. Physiol. 183*, 145−154.
2. Trinh, B. N., Long, T. I., Nickel, A. E., Shibata, D., and Laird, P. W. (2002) DNA methyltransferase deficiency modifies cancer susceptibility in mice lacking DNA mismatch repair, *Mol. Cell. Biol. 22*, 2906−2917.
3. Kane, M. F., Loda, M., Gaida, G. M., Lipman, J., Mishra, R., Goldman, H., Jessup, J. M., and Kolodner, R. (1997) Methylation of the hMLH1 promoter correlates with lack of expression of hMLH1 in sporadic colon tumors and mismatch repair-defective human tumor cell lines, *Cancer Res. 57*, 808−811.
4. El-Osta, A. (2003) DNMT cooperativity − the developing links between methylation, chromatin structure and cancer, *BioEssays 25*, 1071−1084.

5. Bestor, T. H. (2000) The DNA methyltransferases of mammals, *Hum. Mol. Genet. 9*, 2395−2402.
6. Jeltsch, A. (2002) Beyond Watson and Crick: DNA methylation and molecular enzymology of DNA methyltransferases, *ChemBioChem. 3*, 274−293.
7. Hermann, A., Gowher, H., and Jeltsch, A. (2004) Biochemistry and biology of mammalian DNA methyltransferases, *Cell. Mol. Life Sci. 61*, 2571−2587.
8. Das, P. M., and Singal, R. (2004) DNA methylation and cancer, *J. Clin. Oncol. 22*, 4632−4642.
9. Esteller, M. (2005) Aberrant DNA methylation as a cancer-inducing mechanism, *Annu. Rev. Pharmacol. Toxicol. 45*, 629−656.
10. Pfeifer, G. P., Denissenko, M. F., Olivier, M., Tretyakova, N., Hecht, S. S., and Hainaut, P. (2002) Tobacco smoke carcinogens, DNA damage and p53 mutations in smoking-associated cancers, *Oncogene 21*, 7435−7451.
11. Hemminki, K., Koskinen, M., Rajaniemi, H., and Zhao, C. (2000) DNA adducts, mutations, and cancer 2000, *Regul. Toxicol. Pharmacol. 32*, 264−275.
12. Phillips, D. H. (1983) Fifty years of benzo(*a*)pyrene, *Nature 303*, 468−472.
13. Buening, M. K., Wislocki, P. G., Levin, W., Yagi, H., Thakker, D. R., Akagi, H., Koreeda, M., Jerina, D. M., and Conney, A. H. (1978) Tumorigenicity of the optical enantiomers of the diastereomeric benzo[*a*]pyrene 7,8-diol-9,10-epoxides in newborn mice: exceptional activity of (+)-7beta,8alpha-dihydroxy-9alpha,-10alpha-epoxy-7,8,9,10-tetrahydrobenzo[*a*]pyrene, *Proc. Natl. Acad. Sci. U.S.A. 75*, 5358−5361.
14. Weinstein, I. B., Jeffrey, A. M., Jennette, K. W., Blobstein, S. H., Harvey, R. G., Harris, C., Autrup, H., Kasai, H., and Nakanishi, K. (1976) Benzo(*a*)pyrene diol epoxides as intermediates in nucleic acid binding in vitro and in vivo, *Science 193*, 592−595.
15. Wood, R. D. (1999) DNA damage recognition during nucleotide excision repair in mammalian cells, *Biochimie 81*, 39−44.
16. Hess, M. T., Gunz, D., Luneva, N., Geacintov, N. E., and Naegeli, H. (1997) Base pair conformation-dependent excision of benzo-[*a*]pyrene diol epoxide-guanine adducts by human nucleotide excision repair enzymes, *Mol. Cell. Biol. 17*, 7069−7076.
17. Tian, L., Sayer, J. M., Kroth, H., Kalena, G., Jerina, D. M., and Shuman, S. (2003) Benzo[*a*]pyrene-dG adduct interference illuminates the interface of vaccinia topoisomerase with the DNA minor groove, *J. Biol. Chem. 278*, 9905−9911.
18. Choi, D. J., Roth, R. B., Liu, T., Geacintov, N. E., and Scicchitano, D. A. (1996) Incorrect base insertion and prematurely terminated transcripts during T7 RNA polymerase transcription elongation past benzo[*a*]pyrenediol epoxide-modified DNA, *J. Mol. Biol. 264*, 213-219.
19. Chiapperino, D., Kroth, H., Kramarczuk, I. H., Sayer, J. M., Masutani, C., Hanaoka, F., Jerina, D. M., and Cheh, A. M. (2002) Preferential misincorporation of purine nucleotides by human DNA polymerase η opposite benzo[*a*]pyrene 7,8-diol 9,10-epoxide deoxyguanosine adducts, *J. Biol. Chem. 277*, 11765−11771.
20. Rechkoblit, O., Zhang, Y., Guo, D., Wang, Z., Amin, S., Krzeminsky, J., Louneva, N., and Geacintov, N. E. (2002) *Trans*-lesion synthesis past bulky benzo[*a*]pyrene diol epoxide N2-dG and N6-dA lesions catalyzed by DNA bypass polymerases, *J. Biol. Chem. 277*, 30488−30494.
21. MacLeod, M. C., Powell, K. L., Kuzmin, V. A., Kolbanovskiy, A., and Geacintov, N. E. (1996) Interference of benzo[*a*]pyrene diol epoxide-deoxyguanosine adducts in a GC box with binding of the transcription factor Sp1, *Mol. Carcinog. 16*, 44−52.
22. MacLeod, M. C., Powell, K. L., and Tran, N. (1995) Binding of the transcription factor, Sp1, to non-target sites in DNA modified by benzo[*a*]pyrene diol epoxide, *Carcinogenesis 16*, 975−983.
23. Persson, A. E., Ponten, I., Cotgreave, I., and Jernstrom, B. (1996) Inhibitory effects on the DNA binding of AP-1 transcription factor to an AP-1 binding site modified by benzo[*a*]pyrene 7,8-dihydrodiol 9,10-epoxide diastereomers, *Carcinogenesis 17*, 1963−1969.
24. Rechkoblit, O., Krzeminsky, J., Amin, S., Jernstroem, B., Louneva, N., and Geacintov, N. E. (2001) Influence of bulky polynuclear carcinogen lesions in a TATA promoter sequence on TATA binding protein-DNA complex formation, *Biochemistry 40*, 5622−5632.
25. Denissenko, M. F., Chen, J. X., Tang, M. S., and Pfeifer, G. P. (1997) Cytosine methylation determines hot spots of DNA damage in the human P53 gene, *Proc. Natl. Acad. Sci. U.S.A. 94*, 3893−8389.
26. Chen, J. X., Zheng, Y., West, M., and Tang, M. S. (1998) Carcinogens preferentially bind at methylated CpG in the p53 mutational hot spots, *Cancer Res. 58*, 2070−2075.
27. Weisenberger, D. J., and Romano, L. J. (1999) Cytosine methylation in a CpG sequence leads to enhanced reactivity with benzo-[*a*]pyrene diol epoxide that correlates with a conformational change, *J. Biol. Chem. 274*, 23948−23955.
28. Wojciechowski, M. F., and Meehan, T. (1984) Inhibition of DNA methyltransferases *in vitro* by benzo[*a*]pyrene diol epoxide-modified substrates, *J. Biol. Chem. 259*, 9711−9716.
29. Ruchirawat, M., Becker, F. F., and Lapeyre, J.-N. (1984) Mechanism of rat liver DNA methyltransferase interaction with *anti*-benzo[*a*]pyrenediol epoxide modified DNA templates, *Biochemistry 23*, 5426−5432.
30. Wilson, V. L., and Jones, P. A. (1983) Inhibition of DNA methylation by chemical carcinogens in vitro, *Cell 32*, 239−246.
31. Wilson, V. L., and Jones, P. A. (1984) Chemical carcinogen-mediated decreases in DNA 5-methylcytosine content of BALB/3T3 cells, *Carcinogenesis 5*, 1027−1031.
32. Baskunov, V. B., Subach, F. V., Kolbanovskiy, A., Kolbanovskiy, M., Eremin, S. A., Johnson, F., Bonala, R., Geacintov, N. E., and Gromova E. S. (2005) Effects of benzo[*a*]pyrene-deoxyguanosine lesions on DNA methylation catalyzed by EcoRII DNA methyltransferase and on DNA cleavage effected by EcoRII restriction endonuclease, *Biochemistry 44*, 1054−1066.
33. Malone, C. S., Miner, M. D., Doerr, J. R., Jackson, J. P., Jacobsen, S. E., Wall, R., and Teitell, M. (2001) CmC(A/T)GG DNA methylation in mature B cell lymphoma gene silencing, *Proc. Natl. Acad. Sci. U.S.A. 98*, 10404−10409.
34. Gowher, H., and Jeltsch, A. (2001) Enzymatic properties of recombinant Dnmt3a DNA methyltransferase from mouse: the enzyme modifies DNA in a nonprocessive manner and also methylates non-CpG [correction of non-CpA] sites, *J. Mol. Biol. 309*, 1201−1208.
35. Wu, J. C., and Santi, D. V. (1987) Kinetic and catalytic mechanism of HhaI methyltransferase, *J. Biol. Chem. 262*, 4778−4786.
36. Bestor, T. H, and Verdine, G. L. (1994) DNA methyltransferases, *Curr. Opin. Cell. Biol. 6*, 380−389.
37. Renbaum, P., Abrahamove, D., Fainsod, A., Wilson, G. G., Rottem, and S., Razin, A. (1990) Cloning, characterization, and expression in *Escherichia coli* of the gene coding for the CpG DNA methylase from Spiroplasma sp. strain MQ1(M.SssI), *Nucleic Acids Res. 18*, 1145−1152.
38. Pradhan, S., and Roberts, R. J. (2000) Hybrid mouse-prokaryotic DNA (cytosine-5) methyltransferases retain the specificity of the parental C-terminal domain, *EMBO J. 19*, 2103−2114.
39. Koudan, E. V., Bujnicki, J. M., and Gromova, E. S. (2004) Homology modeling of the CG-specific DNA methyltransferase SssI and its complexes with DNA and AdoHcy, *J. Biomol. Struct. Dyn. 22*, 339−345.
40. Sankpal, U. T., and Rao, D. N. (2002) Structure, function, and mechanism of HhaI DNA methyltransferases, *Crit. Rev. Biochem. Mol. Biol. 37*, 167−197.
41. Klimasauskas, S., Kumar, S., Roberts, R. J., and Cheng, X. (1994) HhaI methyltransferase flips its target base out of the DNA helix, *Cell 76*, 357−369.
42. Horton, J. R., Ratner, G., Banavali, N. K., Huang, N., Choi, Y., Maier, M. A., Marquez, V. E., MacKerell, A. D. Jr., and Cheng, X. (2004) Caught in the act: visualization of an intermediate in the DNA base-flipping pathway induced by HhaI methyltransferase, *Nucleic Acids Res. 32*, 3877−3886.
43. Lindstrom, W. M. Jr., Flynn, J., and Reich, N. O. (2000) Reconciling structure and function in HhaI DNA cytosine-C-5 methyltransferase, *J. Biol. Chem. 275*, 4912−4919.
44. Vilkaitis, G., Merkiene, E., Serva, S., Weinhold, E., and Klimasauskas, S. (2001) The mechanism of DNA cytosine-5 methylation. Kinetic and mutational dissection of HhaI methyltransferase, *J. Biol. Chem. 276*, 20924−20934.
45. Daujotyte, D., Serva, S., Vilkaitis, G., Merkiene, E., Venclovas, C., and Klimasauskas, S. (2004) HhaI DNA methyltransferase uses the protruding Gln237 for active flipping of its target cytosine, *Structure 12*, 1047−1055.
46. Huang, N, Banavali, N. K., and MacKerell, A. D. Jr. (2003) Protein-facilitated base flipping in DNA by cytosine-5-methyltransferase, *Proc. Natl. Acad. Sci. U.S.A. 100*, 68−73.
47. Johnson, F., Bonala, R., Tawde, D., Torres, M. C., and Iden, C. R. (2002) Efficient synthesis of the benzo[*a*]pyrene metabolic

adducts of 2′-deoxyguanosine and 2′-deoxyadenosine and their direct incorporation into DNA, *Chem. Res. Toxicol. 15*, 1489−1494.
48. Cantor, C. R., Warshaw, M. M., and Shapiro, H. (1970) Oligonucleotide interactions. 3. Circular dichroism studies of the conformation of deoxyoligonucleotides, *Biopolymers 9*, 1059−1077.
49. Karyagina, A., Shilov, I., Tashlitskii, V., Khodoun, M., Vasil′ev, S., Lau, P. C., and Nikolskaya, I. (1997) Specific binding of SsoII DNA methyltransferase to its promoter region provides the regulation of SsoII restriction-modification gene expression, *Nucleic Acids Res. 25*, 2114−2120.
50. Reid, S. L., Parry, D., Liu, H. H., and Connolly, B. A., (2001) Binding and recognition of GATATC target sequences by the EcoRV restriction endonuclease: a study using fluorescent oligonucleotides and fluorescence polarization, *Biochemistry 40*, 2484−2494.
51. Gowher, H., and Jeltsch, A. (2000) Molecular enzymology of the EcoRV DNA-(Adenine-N (6))-methyltransferase: kinetics of DNA binding and bending, kinetic mechanism and linear diffusion of the enzyme on DNA, *J. Mol. Biol. 303*, 93−110.
52. Brennan, C. A., Van Cleve, M. D., and Gumport, R. I. (1986) The effects of base analogue substitutions on the methylation by the EcoRI modification methylase of octadeoxyribonucleotides containing modified EcoRI recognition sequences, *J. Biol. Chem. 261*, 7279−7286.
53. Subach, O. M., Khoroshaev, A. V., Gerasimov, D. N., Baskunov, V. B., Shchyolkina, A. K., and Gromova, E. S. (2004) 2-Pyrimidinone as a probe for studying the EcoRII DNA methyltransferase-substrate interaction, *Eur. J. Biochem. 271*, 2391−2399.
54. Renbaum, P., and Razin, A. (1995) Footprint analysis of M.Sssl and M.Hhal methyltransferases reveals extensive interactions with the substrate DNA backbone, *J. Mol. Biol. 248*, 19−26.
55. Wyszynski, M. W., Gabbara, S., Kubareva, E. A., Romanova, E. A., Oretskaya, T. S., Gromova, E. S., Shabarova, Z. A., and Bhagwat, A. S. (1993) The cysteine conserved among DNA cytosine methylases is required for methyl transfer, but not for specific DNA binding, *Nucleic Acids Res. 21*, 295−301.
56. Klimasauskas, S., and Roberts, R. J. (1995) M.HhaI binds tightly to substrates containing mismatches at the target base, *Nucleic Acids Res. 23*, 1388−1395.
57. Lin, S. Y., and Riggs A. D. (1972) Lac repressor binding to nonoperator DNA: detailed studies and a comparison of equilibrium and rate competition methods, *J. Mol. Biol. 72*, 671−90.
58. Estabrook, R. A., Lipson, R., Hopkins, B., and Reich, N. (2004) The coupling of tight DNA binding and base flipping: identification of a conserved structural motif in base flipping enzymes, *J. Biol. Chem. 279*, 31419−31428.
59. Geacintov, N. E., Cosman, M., Hingerty, B. E., Amin, S., Broyde, S., and Patel, D. J. (1997) NMR solution structures of stereoisometric covalent polycyclic aromatic carcinogen-DNA adduct: principles, patterns, and diversity, *Chem. Res. Toxicol. 10*, 111−146.
60. Cosman, M., de los Santos, C., Fiala, R., Hingerty, B. E., Singh, S. B., Ibanez, V., Margulis, L. A., Live, D., Geacintov, N. E., and Broyde, S. (1992) Solution conformation of the major adduct between the carcinogen (+)-*anti*-benzo[*a*]pyrene diol epoxide and DNA, *Proc. Natl. Acad. Sci. U.S.A. 89*, 1914−1918.
61. de los Santos, C., Cosman, M., Hingerty, B. E., Ibanez, V., Margulis, L. A., Geacintov, N. E., Broyde, S., and Patel, D. J. (1992) Influence of benzo[*a*]pyrene diol epoxide chirality on solution conformations of DNA covalent adducts: the (−)-trans-anti-[BP]G·C adduct structure and comparison with the (+)-trans-anti-[BP]G·C enantiomer, *Biochemistry 31*, 5245−5252.
62. Lee, C. H., Chandani, S., and Loechler, E. L. (2002) Molecular modeling of four stereoisomers of the major B[*a*]PDE adduct (at N(2)-dG) in five cases where the structure is known from NMR studies: molecular modeling is consistent with NMR results, *Chem. Res. Toxicol. 15*, 1429−1444.
63. Xie, X. M., Geacintov, N. E., and Broyde, S. (1999) Origins of conformational differences between cis and trans DNA adducts derived from enantiomeric anti-benzo[*a*]pyrene diol epoxides, *Chem. Res. Toxicol. 12*, 597−609.
64. Svedruzic, Z. M., Reich, N. O. (2004) The mechanism of target bare attack in DNA cytosine carbon 5 methylation, *Biochemistry 43*, 11460−11473.
65. Renbaum, P., and Razin, A. (1995) Interaction of M.SssI and M.HhaI with single-base mismatched oligodeoxynucleotide duplexes, *Gene 157*, 177−179.
66. Yan, S., Wu, M., Patel, D. J., Geacintov, N. E., and Broyde, S. (2003) Simulating structural and thermodynamic properties of carcinogen-damaged DNA, *Biophys. J. 84*, 2137−2148.
67. Marky, L. A., Kupke, D. W., and Kankia, B. I. (2001) Volume changes accompanying interaction of ligands with nucleic acids, *Methods Enzymol. 340*, 149−165.
68. Tsao, H., Mao, B., Zhuang, P., Xu, R., Amin, S., and Geacintov, N. E. (1998) Sequence dependence and characteristics of bends induced by site-specific polynuclear aromatic carcinogen-deoxyguanosine lesions in oligonucleotides, *Biochemistry 37*, 4993−5000.
69. Huang, X., Colgate, K. C., Kolbanovskiy, A., Amin, S., and Geacintov, N. E. (2002) Conformational changes of a benzo[*a*]-pyrene diol epoxide-N(2)-dG adduct induced by a 5′-flanking 5-methyl-substituted cytosine in a (Me)CG double-stranded oligonucleotide sequence context, *Chem. Res. Toxicol. 15*, 438−444.
70. Zhang, N., Lin, C., Huang, X., Kolbanovskiy, A., Hingerty, B. E., Amin, S., Broyde, S., Geacintov, N. E., and Patel, D. J. (2005) Methylation of cytosine at C5 in a CpG sequence context causes a conformational switch of a benzo[*a*]pyrene diol epoxide-N2-guanine adduct in DNA from a minor groove alignment to intercalation with base displacement, *J. Mol. Biol. 346*, 951−965.
71. O'Gara, M., Klimasauskas, S., Roberts, R. J., and Cheng, X. (1996) Enzymatic C5-cytosine methylation of DNA: mechanistic implications of new crystal structures for HhaL methyltransferase-DNA-AdoHcy complexes, *J. Mol. Biol. 261*, 634−645.
72. Marnett, L. J., Riggins, J. N., and West, J. D. (2003) Endogenous generation of reactive oxidants and electrophiles and their reactions with DNA and protein, *J. Clin. Invest. 111*, 583−593.
73. De Bont, R., and van Larebeke, N. (2004) Endogenous DNA damage in humans: a review of quantitative data, *Mutagenesis 19*, 169−185.
74. Greenberg,M. M. (2004) In vitro and in vivo effects of oxidative damage to deoxyguanosine, *Biochem. Soc. Trans. 32*, 46−50.
75. Turk, P. W., Laayoun, A., Smith, S. S., and Weitzman, S. A. (1995) DNA adduct 8-hydroxyl-2′-deoxyguanosine (8-hydroxyguanine) affects function of human DNA methyltransferase, *Carcinogenesis 16*, 1253−1255.
76. Tan, N. W., and Li, B. F. (1990) Interaction of oligonucleotides containing 6-O-methylguanine with human DNA (cytosine-5)-methyltransferase, *Biochemistry 29*, 9234−9240.
77. Smith, S. S., Kan, J. L., Baker, D. J., Kaplan, B. E., and Dembek, P. (1991) Recognition of unusual DNA structures by human DNA (cytosine-5)methyltransferase, *J. Mol. Biol. 217*, 39−51.
78. Perera, F. P., Tang, D., Tu, Y. H., Cruz, L. A., Borjas, M., Bernert, T., and Whyatt, R. M. (2004) Biomarkers in maternal and newborn blood indicate heightened fetal susceptibility to procarcinogenic DNA damage, *Environ. Health Perspect. 112*, 1133−1136.
79. Everson, R. B., Randerath, E., Avitts, T. A., Schut, H. A., and Randerath, K. (1987) Preliminary investigations of tissue specificity, species specificity, and strategies for identifying chemicals causing DNA adducts in human placenta, *Prog. Exp. Tumor Res. 31*, 86−103.
80. Shugart, L. R. (1988) Quantification of chemically induced damage to DNA of aquatic organisms by alkaline unwinding assay, *Aquat. Toxicol. 13*, 43−52.
81. Hainaut, P., and Pfeifer, G. P. (2001) Patterns of p53 G→T transversions in lung cancers reflect the primary mutagenic signature of DNA-damage by tobacco smoke, *Carcinogenesis 22*, 367−374.
82. Bos, J. L. (1989) ras oncogenes in human cancer: a review, *Cancer Res. 49*, 4682−4689.
83. Wilson, W. L., Smith, R. A., Longoria, J., Liotta, M. A., Harper, C. M., and Harris, C. C. (1987) Chemical carcinogen-induced decreases in genomic 5-methyldeoxycytidine content of normal human bronchial epithelial cells, *Proc. Natl. Acad. Sci. U.S.A. 84*, 3298−3301.
84. Gowher, H., Liebert, K., Hermann, A., Xu, G., and Jeltsch, A. (2005) Mechanism of stimulation of catalytic activity of Dnmt3A and Dnmt3B DNA-(cytosine-C5)-methyltransferases by Dnmt3L, *J. Biol. Chem. 280*, 13341−13348.
85. Conney, A. H. (1982) Induction of microsomal enzymes by foreign chemicals and carcinogenesis by polycyclic aromatic hydrocarbons: G. H. A. Clowes Memorial Lecture, *Cancer Res. 42*, 4875−4917.

BI0511639